

dy-09113

N 70 15992  
REPORT NO.: 2370

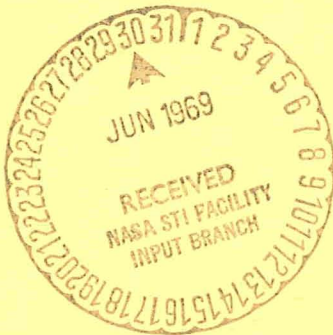
CONTRACT NO.: NAS8-20832

DATE: JANUARY 27, 1969

NASA CR 102388

FINAL REPORT  
FOR  
APPLIED RESEARCH AND FEASIBILITY STUDIES,  
EXPERIMENTAL INVESTIGATIONS AND CONCEPTUAL  
OR PRELIMINARY DESIGN ENGINEERING APPLI-  
CABLE TO INVERTERS FOR MOTORS PROGRAM.

(JUNE 1967 TO JANUARY 1969)



PREPARED BY  
GULTON INDUSTRIES, INC.  
Engineered Magnetics Division  
13041 Cerise Avenue  
Hawthorne, California

FOR  
NATIONAL AERONAUTICS AND SPACE ADMINISTRATION  
MARSHALL SPACE FLIGHT CENTER  
HUNTSVILLE, ALABAMA

**CASE FILE  
COPY**

**Gulton Industries, Inc.**



ENGINEERED MAGNETICS DIVISION • 13041 CERISE AVE., HAWTHORNE, CALIF.

REPORT NO.: 2370

CONTRACT NO.: NAS8-20832

DATE: JANUARY 27, 1969

FINAL REPORT  
FOR  
APPLIED RESEARCH AND FEASIBILITY STUDIES,  
EXPERIMENTAL INVESTIGATIONS AND CONCEPTUAL  
OR PRELIMINARY DESIGN ENGINEERING APPLI-  
CABLE TO INVERTERS FOR MOTORS PROGRAM.

(JUNE 1967 TO JANUARY 1969)

SUBMITTED BY:

D. B. Irvine  
D. B. Irvine  
Project Engineer

REVIEWED BY:

J. W. Bates  
J. W. Bates  
Product Manager

APPROVED BY:

B. G. McComb  
B. G. McComb  
Vice President  
Engineered Magnetics  
Division

PREPARED BY  
GULTON INDUSTRIES, INC.  
Engineered Magnetics Division  
13041 Cerise Avenue  
Hawthorne, California  
FOR  
NATIONAL AERONAUTICS AND SPACE ADMINISTRATION  
MARSHALL SPACE FLIGHT CENTER  
HUNTSVILLE, ALABAMA

## ABSTRACT

This report presents the results of the Applied Research and Feasibility Studies, Experimental Investigations and Conceptual or Preliminary Design Engineering Applicable to Inverters for Motors Study Program. The Study Program conducted by Engineered Magnetics from June 1967 to January 1969 was based on information derived from the Inverters For Motors Study Program (NASA Contract No. NAS8-18013, Engineered Magnetics Final Report No. 2068), conducted by Engineered Magnetics from June 1966 to June 1967.

During this study program, an inverter-motor system was developed and used to obtain information relating to efficiency, torque versus speed, slip control, current limiting, and design and operating characteristics of inverters and motors. The information obtained during the study program is presented in this report. The inverter-motor system consisted of a 1/7 horsepower rated AC induction type motor operated in conjunction with an inverter breadboard having a quasi-square wave output. The motor was fabricated and tested in accordance with design requirements defined by Engineered Magnetics. The inverter breadboard was designed and fabricated by Engineered Magnetics Division of Gulton Industries.

## TABLE OF CONTENTS

	PAGE NO.
PREFACE	1
SUMMARY	2
I. INTRODUCTION	5
II. INVERTER-MOTOR APPLICATIONS	6
III. MOTOR ANALYSIS AND INVERTER DESIGN REVIEW	8
A. Motor Analysis	8
B. Inverter Design Review	15
IV. SYSTEM TEST	37
A. Inverter Breadboard Design and Test Results	37
B. Motor Design and Test Results	53
V. CONCLUSIONS	66
APPENDIX I. FINAL INVERTER DESIGN (THREE PHASE QUASI-SQUARE WAVE OUTPUT) AND LIST OF MATERIAL	
APPENDIX II. BLOCK DIAGRAM OF INVERTER BREADBOARD	

### LIST OF FIGURES

FIGURE 1. THREE PHASE QUASI-SQUARE WAVE INVERTER RING COUNTER	16
FIGURE 2. THREE PHASE QUASI-SQUARE WAVE GATING CIRCUIT	18
FIGURE 3. SIX PHASE HALF WAVE INVERTER WAVEFORMS TO GENERATE QUASI-SQUARE WAVEFORMS, USING RING COUNTER AND GATING CIRCUIT	20
FIGURE 4. SIX PHASE HALF WAVE QUASI-SQUARE WAVE INVERTER USING RING COUNTER AND GATING CIRCUIT	21
FIGURE 5. GENERATION OF PULSE WIDTH MODULATED WAVEFORM FOR CURRENT LIMITING	24
FIGURE 6. WAVESHAPES OF $e_n$ WITH $6f_0$ PULSE WIDTH	25
FIGURE 7. WAVESHAPES OF $e_n$ WITH $12f_0$ PULSE WIDTH	26
FIGURE 8. WAVESHAPES OF $e_n$ WITH $24f_0$ PULSE WIDTH	27

	LIST OF FIGURES (CONT'D)	PAGE NO.
FIGURE 9.	PULSE TIMING WAVEFORMS	31
FIGURE 10.	TEST SETUP WITH PULSE WIDTH CURRENT SENSING AND LIMITING CIRCUIT (PRELIMINARY DESIGN)	38
FIGURE 11.	OSCILLOSCOPE PHOTOGRAPHS 1, 2, AND 3.	39
FIGURE 12.	OSCILLOSCOPE PHOTOGRAPHS 4, 5, AND 6	40
FIGURE 13.	OSCILLOSCOPE PHOTOGRAPHS 7, 8, AND 9	41
FIGURE 14.	TEST SETUP WITH REVISED PULSE WIDTH CURRENT SENSING AND LIMITING CIRCUIT (FINAL DESIGN)	43
FIGURE 15.	CONSTANT SLIP-FIXED FREQUENCY	44
FIGURE 16.	MOTOR SPEED, TORQUE, AND INPUT CURRENT 3 AMPS NOMINAL (SLIP:25 Hz)	45
FIGURE 17.	MOTOR SPEED, TORQUE, AND INPUT CURRENT 6.5 AMPS NOMINAL (SLIP:25Hz)	46
FIGURE 18.	MOTOR TORQUE AND INPUT CURRENT 5 AMPS NOMINAL (SLIP:25Hz)	47
FIGURE 19.	MOTOR TORQUE-SPEED: 2.4 AMPS STARTING CURRENT (SLIP:25Hz)	49
FIGURE 20.	MOTOR TORQUE-SPEED: 5 AMPS AT STALL, 30 VOLTS INPUT (SLIP:25Hz)	50
FIGURE 21.	MOTOR TORQUE-SPEED: 5 AMPS AT STALL, 35 VOLTS INPUT (SLIP:25Hz)	51
FIGURE 22.	MOTOR TORQUE-SPEED (SLIP:8 1/3 Hz)	54
FIGURE 23.	MOTOR TORQUE-SPEED (SLIP:16 2/3 Hz)	55
FIGURE 24.	MOTOR TORQUE-SPEED (SLIP:33 1/3 Hz)	56
FIGURE 25.	MOTOR NO. 1 PERFORMANCE CURVES (MANUFACTURERS DATA)	58
FIGURE 26.	MOTOR NO. 2 PERFORMANCE CURVES (MANUFACTURERS DATA)	59
FIGURE 27.	SIX PHASE MOTOR INPUT TEST CONNECTIONS	60
FIGURE 28.	EFFICIENCY VS SLIP:6Ø SQUARE WAVE AND 6Ø QUASI- SQUARE WAVE	61
FIGURE 29.	MOTOR TORQUE-SPEED, INVERTER OUTPUT FILTERED (SLIP:20Hz)	63
FIGURE 30.	MOTOR TORQUE-SPEED, INVERTER OUTPUT NOT FILTERED (SLIP:20Hz)	64
FIGURE 31.	INVERTER OUTPUT PHOTOGRAPHS	65

## PREFACE

This is the Final Report of Engineered Magnetics Applied Research and Feasibility Studies, Experimental Investigations and Conceptual or Preliminary Design Engineering Applicable To Inverters For Motors Study Program.

This Final Report is for the contract period of June 1967 to January 1969. During the course of the contract, technical monthly and quarterly progress reports were prepared and submitted to NASA.

## SUMMARY

The National Aeronautics and Space Administration Contract Number NAS8-20832, Applied Research and Feasibility Studies, Experimental Investigations and Conceptual or Preliminary Design Engineering Applicable To Inverters For Motors Program (here-in after referred to as the "Study Of Inverters Program"), was awarded to the Engineered Magnetics Division of Gulton Industries, Inc., in June 1967.

The Study of Inverters Program was conducted at Engineered Magnetics Division from June 1967 to December 1968. The objectives of the Study of Inverters Program are defined as follows:

1. Develop advanced inverters with higher efficiency and improved performance characteristics required for motor operation that will assure the improved reliability and long life required for space vehicle applications.
2. Advance technology in the field of power conditioning with improved design concepts and techniques.
3. Effect the necessary improvements in materials, components, and processes required to achieve maximum performance and reliability.
4. Consider general systems requirements such as ruggedness, simplicity, ease of operation, and maintainability in accomplishing the prime objectives.

During the Study of Inverters Program, several motor and inverter designs were investigated in order to determine which motor and inverter types are most compatible when connected as an inverter-motor combination. The Motor Analysis and Inverter Design Review portion of the study resulted in the selection of an AC induction type motor to be operated by a quasi-square wave inverter output. The selection of the motor was accomplished after analyzing the characteristics and requirements of synchronous and induction type motors. Motors operating on DC inputs were not included in the Study Program because of the inherent inadequacies and noise generating characteristics of this motor type

The excited synchronous motor which contains slip rings and brushes was also excluded from further study. This type of motor was determined to be undesirable for the Study of Inverters Program due to the excessive motor size and weight required to obtain a useable horsepower rating.

The induction motor presents the most desirable characteristics for a general purpose (airborne) application. The operating characteristics of the induction motor were analyzed in detail to establish the basic inverter requirements for AC motor operation.

Inverter output characteristics were studied and the quasi-square wave inverter output was selected as the most adaptable for operating the AC motor. The quasi-square wave, which more nearly duplicates a sine wave and can easily be formed to operate an AC motor was selected for intensive investigation. Unlike other inverter designs the quasi-square wave inverter requires no heavy transformer to supply a useable output.

An AC induction type, 1/7 horsepower rated motor consisting of one rotor and two interchangeable field housing assemblies was purchased for the Study Program. The two field housing assemblies were of different material and thus there were, in effect, two different motors having identical rotors, which permitted the affect of material in relation to motor efficiency to be investigated.

#### Design Guidelines

1. In general, the performance and environmental requirements as specified for Saturn-Apollo systems and electronic equipment was used as guideline specifications for the Study of Inverters Program. It is emphasized that this study program attempts to improve performance and also to extend the life and environmental range capability of space vehicle inverters.

2. Special guideline requirements are itemized below:

Input:	28 $\pm$ 4 VDC (for motors less than 3/4 horsepower rating)
Input Deviation:	Motor-Inverter shall operate without damage for 100 hours with input voltage deviations of $\pm$ 15%.
Power:	100 VA to 2 horsepower rating.
Output:	Voltage, frequency, regulation, and wave form to be consistent with required optimum performance and the motor-inverter interface.
Efficiency:	Motor characteristics did not permit 85% efficiency.
Operation Life:	1500 hours.
Overload Protection:	Current limiting circuit designed.

The results of system tests pertain to inverter-motor efficiency, motor torque and slip, and other inverter-motor characteristics when operating as a system.

## I. INTRODUCTION.

Engineered Magnetics received the authority to proceed for the Applied Research and Feasibility Studies, Experimental Investigations, and Conceptual Or Preliminary Design Engineering Applicable to Inverters For Motors (here-in after referred to as the Study of Inverters Program) as stated in the National Aeronautics and Space Administration Contract No. NAS8-20832 dated June 1967.

The major purpose of this study program is to define motor and inverter interface and design requirements that will result in optimum performance and reliability of an inverter-motor system.

This report presents information pertaining to the Study of Inverters Program starting in June 1967, and continuing to January 1969. The information contained here-in relates to the following areas:

- Inverter-Motor Applications.

- Motor Analysis and Inverter Design Review.

- System Tests.

## II. INVERTER-MOTOR APPLICATIONS.

There are several applications for inverter-motor combinations. A few of these applications are discussed in the following paragraphs.

### A. Vehicle Drive.

Inverter-motor applications for vehicle drive include a possible lunar transport vehicle that is designed to carry its prime power (such as batteries or fuel cell). An inverter used for this application will contain circuits for current control, slip frequency control, and motor reversal to permit variable speed operation at maximum system efficiency. A vehicle designed for this purpose will usually be operating at conditions considerably less than maximum speed, while maintaining torque, speed control, and the ability to operate in a reverse direction.

### B. Centrifugal Pump.

A centrifugal pump does not require any inverter control features as the torque is low until the pump approaches its normal operating speed. The inverter for this application will be of a standard design and the impeller motor can have a comparatively high resistance rotor, which will reduce initial in-rush current.

### C. Multi-speed Blower.

The requirements of a multi-speed blower are similar to the centrifugal pump requirements, except motor speed control is obtained by varying the inverter output frequency. This motor speed control technique requires control of the motor input voltage level to prevent saturation of the motor iron when the inverter output frequency is decreased.

### D. Positive Displacement Pump.

A motor driving a positive displacement pump is required to develop a high starting torque. For this requirement, slip frequency control will be used to maintain a high starting torque while limiting current. This system normally functions at the rated speed of the motor, as efficiency at lower speeds is not a requirement of this application.

E. Control Moment Gyro (CMG) Spin Motor.

The requirement for this system is analogous with the vehicle drive requirements. High efficiency at low speed is an important factor in this application.

The CMG spin motor operates at less than full speed for a considerable length of time after starting, due to the long time required for the motor to obtain full speed.

The inverter-motor system applications require motors of the three phase induction type design. The recommended inverter output is either three phase quasi-square wave or six phase, half wave, quasi-square wave configuration.

### III. MOTOR ANALYSIS AND INVERTER DESIGN REVIEW.

#### A. Motor Analysis.

Engineered Magnetics Report No. 2068 (Final Report For Inverters For Motors Study Program, prepared for NASA Contract No. NAS8-18013) presented a review of the characteristics of several types of motors used in applications where high reliability is required. The motor analysis was based on information obtained from several standard books and articles, and from discussions with motor manufacturers. The guidelines of the study program restricted the motor types to be investigated to multiphase motors of relatively low horsepower having no brushes or slip rings. The motor types investigated were synchronous and induction type motors. These motors are designed for use with alternating current. Direct current operated motors were not investigated for the study program because of inherent inadequacies and noise generating characteristics related to this type of motor.

Excited synchronous motors, which require a DC excitation current, were only briefly studied as these motors contain slip rings and brushes, and are, therefore, outside of the scope of the study program. Non-excited synchronous motors, such as synchronous-inductance or hysteresis type motors, were not considered as being practical for large power applications as they are less efficient and larger in size than induction motors of the same power rating.

The induction motor is the type most commonly employed for general purpose applications. An alternating current is applied directly to the stator windings, and supplied by induction to the rotor winding. The performance of induction motors is described in detail, in EMD Report No. 2068, by the use of equivalent circuit illustrations and approximate graphical analysis employing a circle diagram.

Based on the information presented in EMD Report No. 2068, the motor design best qualified for general application is the induction motor with a squirrel cage rotor. The primary problems related to this type of motor are low starting torque and high inrush current when the motor is designed for maximum efficiency operation. Methods of overcoming the low starting torque and high inrush current characteristics of the induction motor and methods of achieving variable speed operation are presented in the following paragraphs.

#### 1. Frequency and Speed.

Heat generation is the major speed limiting factor related to motor design. Gears and gear trains lower system efficiency, except when used in large systems. Therefore, the motor should be matched to the load. This motor-to-load match is accomplished by selecting the necessary number of poles for the motor and inverter frequency.

A frequency of 400 Hz is generally considered the optimum input frequency for motor operation for the following reasons:

- a. Equipment size is reasonably compact.
- b. Increasing the frequency above 400 Hz to reduce motor size results in increased core loss, manufacturing problems related to handling extremely thin motor laminations and fine tolerances, and the requirement for heat removal.

#### 2. Harmonics.

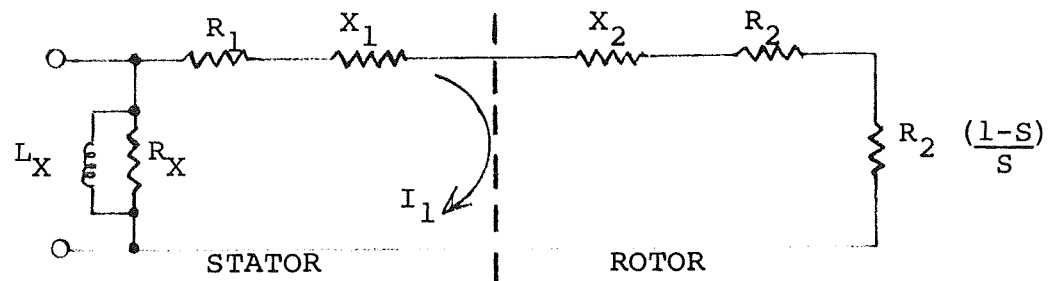
There are two classes of harmonics that detract from motor performance. These harmonics are: (a) space harmonics due to winding restrictions of the stator assembly, and (b) time harmonics caused by the applied voltage not being a pure sine wave. (The harmonics are discussed in detail in EMD Report No. 2068.)

The rotating field produced by time harmonics is above the synchronous speed of the motor. Space harmonics are slower than the synchronous speed of the motor. Motor manufacturers overcome the difficulties caused by space harmonics by "skewing" the rotor (at a slight cost in efficiency), and by winding configuration. The effect of time harmonics is evident in increased core loss, but generally time harmonics have little effect on motor torque-speed curves.

### 3. Variable Speed Operation.

A motor will deliver maximum torque for variable speed operation if the rotor frequency is kept constant ( $\omega_R = k$ ), assuming that the flux density  $(\frac{V}{F})^2$  ratio is constant and the variations of windage and core loss are ignored.

If the following simplified equivalent circuit of a motor is used, the exciting inductance ( $L_X$ ) and core loss ( $R_X$ ) are moved to the input terminals.



Assume:  $X_1 = X_2$  (referred to stator),  $R_1 = R_2 = R$  (referred to stator),  $S$  = slip ratio, the input power will equal  $I_1^2 \left[ R_1 + R_2 + R_2 \left( \frac{1-S}{S} \right) \right] = I^2 R \left( 2 + \frac{1-S}{S} \right)$

and output power will equal  $I_1^2 R_2 \left( \frac{1-S}{S} \right) = I^2 R \left( \frac{1-S}{S} \right)$ .

Efficiency, ignoring core loss ( $R_X$ ) will be:

$$\frac{P_{out}}{P_{in}} = \frac{I^2 R \frac{1-S}{S}}{I^2 R \left( 2 + \frac{1-S}{S} \right)} \times 100\% = \frac{1-S}{1+S} \times 100\%.$$

If the core loss remains fixed at 20% and inverter efficiency is 90%, a 400 Hz - 6 pole motor will give the following calculated performance.

EFFICIENCY WITH MOTOR DESIGNED FOR OPTIMUM PERFORMANCE AT 5% SLIP (20 Hz).

INPUT FREQUENCY (Hz)	MOTOR SPEED (RPM)	SLIP (Hz)	SLIP RATIO	ROTOR EFFICIENCY $\frac{1-S}{1+S} \times 100\%$ (%)	MOTOR EFFICIENCY (CORE LOSS = 20%) (%)	SYSTEM EFFICIENCY (INVERTER=90%) (%)
400	7600	20	.05	90.5	72.4	65.1
300	5600	20	.067	87.3	69.6	62.6
200	3600	20	.10	81.8	65.4	58.9
100	1600	20	.20	66.7	53.4	48.0
50	600	20	.40	42.8	34.2	30.8
40	400	20	.50	33.3	26.6	24.0
30	200	20	.67	20.0	16.0	14.4

EFFICIENCY WITH MOTOR DESIGNED FOR OPTIMUM PERFORMANCE AT 2% SLIP (8 Hz).

INPUT FREQUENCY (Hz)	MOTOR SPEED (RPM)	SLIP (Hz)	SLIP RATIO	ROTOR EFFICIENCY $\frac{1-S}{1+S} \times 100\%$ (%)	MOTOR EFFICIENCY (CORE LOSS = 20%) (%)	SYSTEM EFFICIENCY (INVERTER=90%) (%)
400	7840	8	.02	96.0	76.7	69.1
300	5840	8	.0267	94.8	75.0	67.5
200	3840	8	.04	92.4	73.8	66.4
100	1840	8	.08	85.1	68.0	61.2
50	840	8	.16	72.3	57.7	52.0
40	640	8	.20	66.7	53.4	48.1
30	440	8	.267	57.9	46.3	41.8

The two Efficiency Tables emphasize the necessity of designing a motor for low constant slip operation, if reasonable efficiency is to be obtained. (Note: 20% core loss and 90% inverter efficiency were selected for comparative purposes only.)

See Section IV, paragraph B , for constant slip operation tests.

The equation for variable speed at constant slip frequency consists of the following factors:

$\phi_s$  = Flux due to stator winding

$\phi_r$  = Flux due to rotor winding

$E_1$  = Air gap voltage

$E_2$  = Rotor voltage

$I_2$  = Rotor current

$\omega_{SL}$  = Slip frequency in radians per second.

$\omega_s$  = Input frequency in radians per second

$\omega_2$  = Rotor frequency in radians per second

$\sin \delta$  = Rotor phase angle

If the voltage drop of the stator circuit is not considered then the following relationships are applicable.

$$\phi_s \propto \frac{E_1}{\omega_s} \quad (1)$$

$$\omega_{SL} = \omega_s - \omega_2, \text{ slip} = \frac{\text{synchronous frequency}}{\text{actual frequency}} \quad (2)$$

$$E_2 \propto \phi_s \cdot \omega_{SL} \quad (3)$$

$$I_2 = \frac{E_2}{R_2} \propto \frac{\omega_{SL} \phi_s}{R_2} \quad (X_2 \text{ is not considered}) \quad (4)$$

$$\phi_r \propto \frac{\omega_{SL} \phi_s}{R_2} \quad (5)$$

$$T \propto \phi_s \phi_r \sin \delta \quad (\text{basic torque (T) relationship}) \quad (6)$$

The result of combining (1) and (5) is:

$$T \propto \left(\frac{E_1}{\omega_s}\right)^2 \left(\frac{\omega_{SL}}{R_2}\right) \quad (7)$$

which shows that torque is constant with frequency if the input voltage per Hertz (Hz) is constant and the rotor slip frequency is constant.

But, since the rotor circuit contains inductance ( $L_2$ ), the rotor impedance is:

$$Z_2 = \sqrt{R_2^2 + (\omega_{SL} L_2)^2} \quad (8)$$

The rotor flux lags the stator flux by an angle greater than  $90^\circ$  and the rotor power factor is

$$\phi_2 = \tan^{-1} \left( \frac{\omega_{SL} L_2}{R_2} \right) \quad (9)$$

$$\text{Therefore, } \delta = 90^\circ + \phi_2 \text{ or } \sin \delta = \cos \phi_2 = \frac{R_2}{\sqrt{R_2^2 + (\omega_{SL} L_2)^2}} \quad (10)$$

Torque becomes

$$T \propto \left( \frac{E_1}{\omega_s} \right)^2 \frac{\omega_{SL} R_2}{R_2^2 + (\omega_{SL} L_2)^2} \quad (11)$$

The air gap voltage ( $E_1$ ) is the input voltage minus the stator impedance voltage drop. This torque is independent of input frequency as long as the stator flux ( $\phi_s$ ) is constant and the motor operates at the same slip frequency. (This conclusion ignores the minor variation caused by windage, core loss, and friction with speed.) Differentiation of equation (11) shows that the maximum torque ( $T_{max}$ ) occurs at a slip frequency

$$\omega_{SL} \Big|_{T_{max}} = \omega_m = \frac{R_2}{L_2}, \text{ where } \omega_m \text{ is slip frequency at } T_{max}, \quad (12)$$

or at the maximum torque point ( $R_2 = \omega_m L_2$ ).

To maintain a constant stator flux at low input frequency, the input voltage should be higher than the V/F (voltage to frequency) relationship. The higher voltage is necessary to compensate for copper loss. At higher-than-normal operating frequency the voltage should be higher than predicted by the V/F relationship, to compensate for the increased stator impedance drop, thus maintaining a constant stator flux density as the frequency varies over a wide range.

The voltage-frequency relationship should be somewhat shaped and the amount of correction depends on motor design.

B. Inverter Design Review.

A review of inverter designs is presented in Report No. 2068 (Final Report for the NASA Contract NAS8-18013 Study program). The major inverter designs discussed in the report were square wave, quasi-square wave, and stepped wave(harmonic interchange) inverters. The inverter wave forms were investigated through the use of a Fourier Analysis.

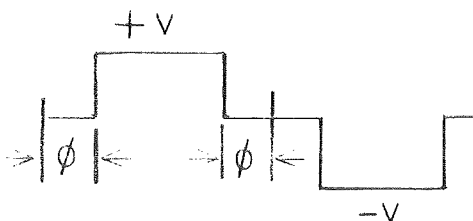
After analyzing inverter characteristics (such as size, weight, efficiency, cost, ease of maintenance, control possibilities, reliability, life expectancy, and stability) the quasi-square wave inverter was selected for further investigation for this study program. This inverter design permits the generation of three phase voltages without requiring output transformers.

Report No. 2068 presents information concerning transformer versus transformerless operation. Based on this information, the transformerless three phase quasi-square wave inverter was the best selection in terms of size, weight, and reliability. One of the objectives of this study program is the investigation of low speed starting and variable speed operation. Therefore, inverter configuration is of major importance in weight sensitive applications.

1. Fourier Analysis.

The following Fourier Analysis is of the Quasi-Square Waveform output of the inverter.

The quasi-square waveform has the following characteristics.



$$f(t) = E(\omega t) = \frac{AV}{\pi} (\cos \phi \sin \omega t + \frac{\cos 3\phi}{3} \sin 3 \omega t + \dots$$

$$\dots + \frac{\cos(2n-1)\phi}{2n-1} \sin (2n-1)\omega t \quad (\omega T = \text{Angular Velocity.})$$

If  $\phi = 30^\circ$ ,  $\cos 3\phi = 0$  and the third and multiples of the third harmonics are zero

#### Summary of the above Fourier Analysis

Harmonic value	Relative voltage
1	100 (%)
3	0
5	20
7	14.28
9	0
11	9.09
13	7.69
15	0.0
17	5.88
19	4.35

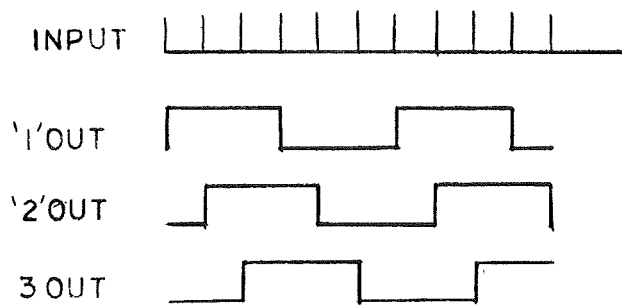
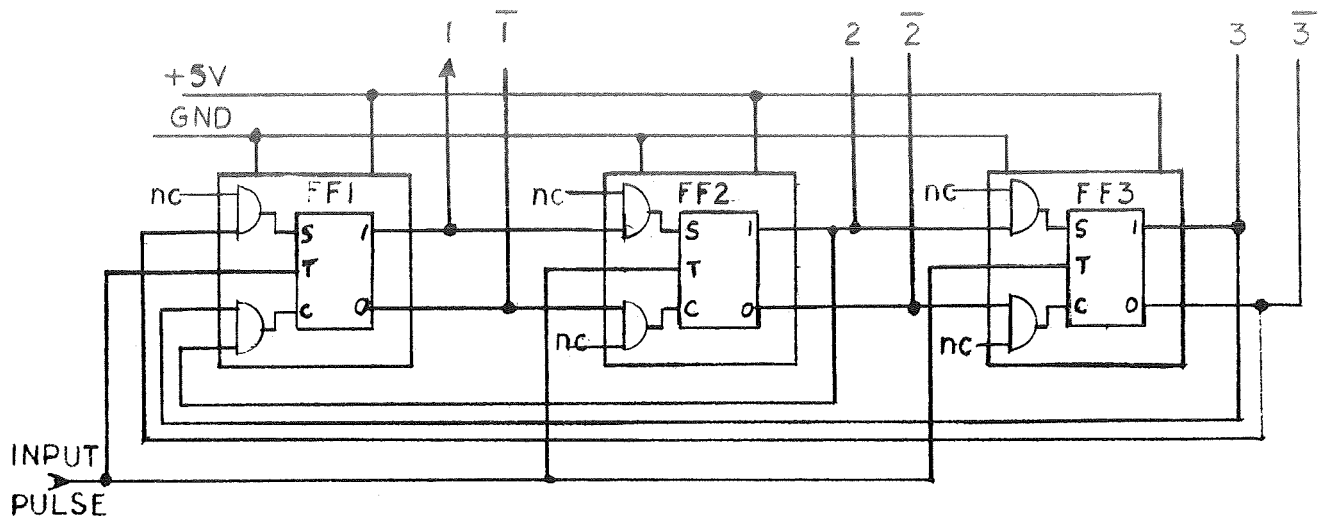
Total harmonic distortion (THD) is 31.1%

## 2. Inverter Output Waveform Generation.

### a. Three phase quasi-square waveform.

This is the simplest waveform that can be used to drive a three phase motor. The inverter circuit used to obtain this output is known as a "Johnson Counter" or "switch-tailed ring counter". A simplified schematic for this inverter is shown on Figure 1. The flipflops are Fairchild type 945 (the direct set and direct clear inputs are not shown as they are not connected in this application). Both 'clear' inputs for FF1 are utilized to prevent the following undesired counting sequence.

COUNT	FF1	FF2	FF3
1	1	0	1
2	0	1	0
3	1	0	1



INPUT	FF1	FF2	FF3
1	1	0	0
2	1	1	0
3	1	1	1
4	0	1	1
5	0	0	1
6	0	0	0
1	1	0	0
2	1	1	0

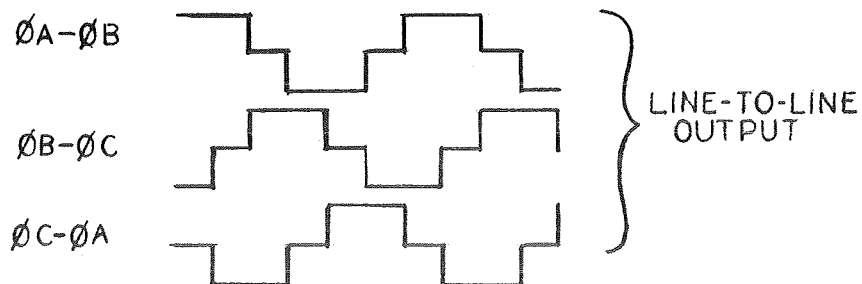
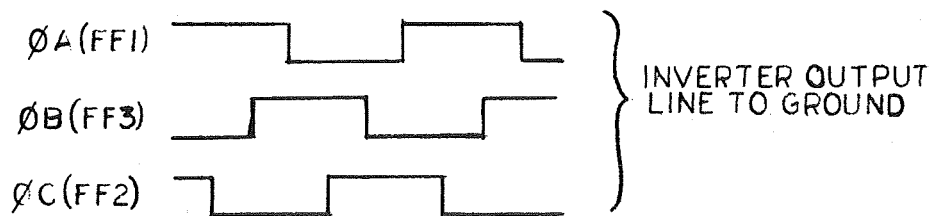


FIGURE 1. THREE PHASE QUASI-SQUARE WAVE INVERTER RING COUNTER.

The flipflop outputs are connected to the inverter through NAND gates. These NAND gates enable rotation control by interchanging phases B and C. The pulse width current control signal is introduced at this point. Figure 2 shows the three phase gating circuit design. This circuit diagram illustrates how the current control signal is applied to all gates, and the method to achieve motor reversal.

b. Six Phase Half Wave Inverter.

The six phase half wave quasi-square wave inverter circuit was investigated. This inverter circuit has the same number of output transistors as the three phase quasi-square wave inverter circuit. The advantages presented by the six phase inverter circuit are:

The output transistors are all connected to the ground side of the motor input. This design simplifies the drive requirement of the inverter.

The possibility of both transistors in one line being on simultaneously due to transistor storage times (which is possible with a conventional three phase inverter circuit  $180^{\circ}$  transistor "on" time) is avoided.

Some disadvantages of the six phase inverter are as follows:

Motor design requirements are considerably more complicated than the requirements for three phase operation. The six phase inverter design requires a motor with bifilar windings and eight leads to the inverter output.

The logic required to generate the final quasi-square wave signals is more complicated in design than for three phase quasi-square wave inverter logic.

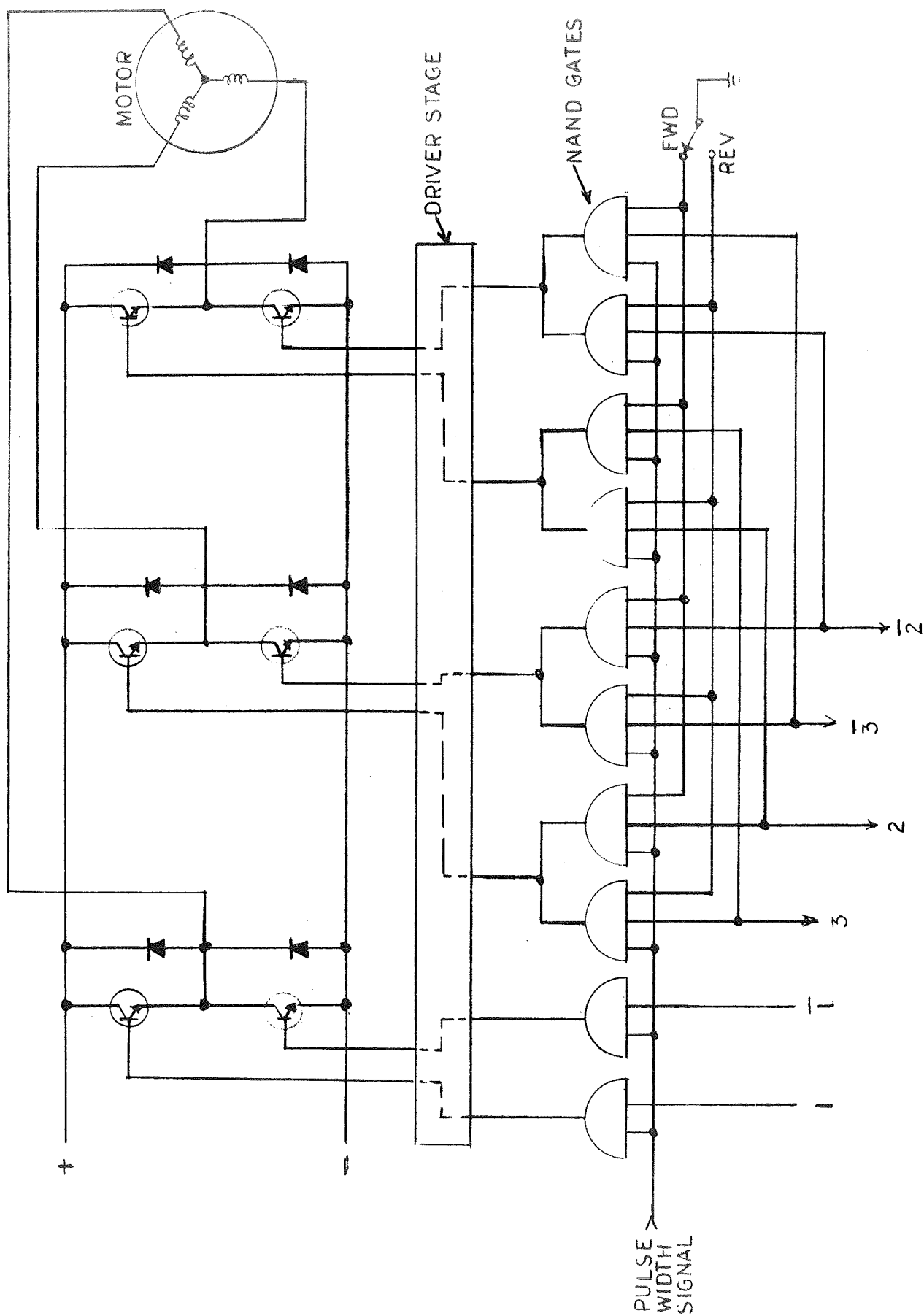


FIGURE 2. THREE PHASE QUASI-SQUAREWAVE GATING CIRCUIT.

Obtaining maximum efficiency may require an interphase transformer.

Figure 3 shows how the quasi-square waveform can be generated from a half waveform by using the same ring counter as shown on Figure 1. Figure 4 shows the physical configuration of this circuit, including facilities for phase rotation control and pulse width current limiting control.

If a three phase bifilar wound motor is driven by six square waves then the logic circuit of Figure 4 can be used. However the interphase transformer shown in Figure 4 will definitely be required to suppress the third harmonic current that could be present with square wave drive. This third harmonic, if present, represents a large amount of wasted power as this harmonic is quite high and does not produce any rotating torque.

Breadboard tests have indicated that the interphase transformer results in slightly improved efficiency even with quasi-square wave drive. This transformer can be comparatively small as the frequency components that it must suppress is 6 times the fundamental with an average value of  $1/3$  the fundamental for square wave drive. In the case of the quasi-square wave drive signal, the transformer will handle, essentially, unbalances due to transistor saturation voltage differences, variations in switching times, and winding resistances. Test data indicates that efficiencies for the six phase, half wave quasi-square wave drive and the three phase full wave quasi-square wave drive are very similar.

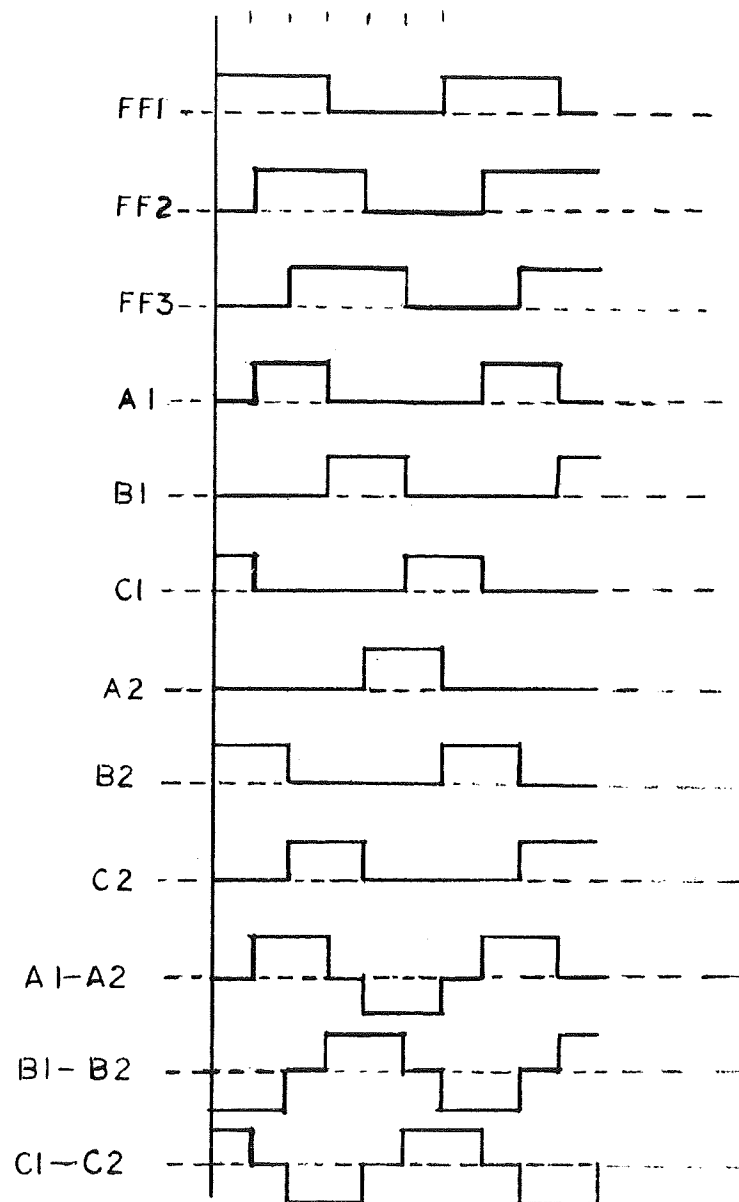


FIGURE 3. SIX PHASE HALF WAVE INVERTER WAVEFORMS TO GENERATE QUASI-SQUARE WAVEFORMS, USING RING COUNTER AND GATING CIRCUIT

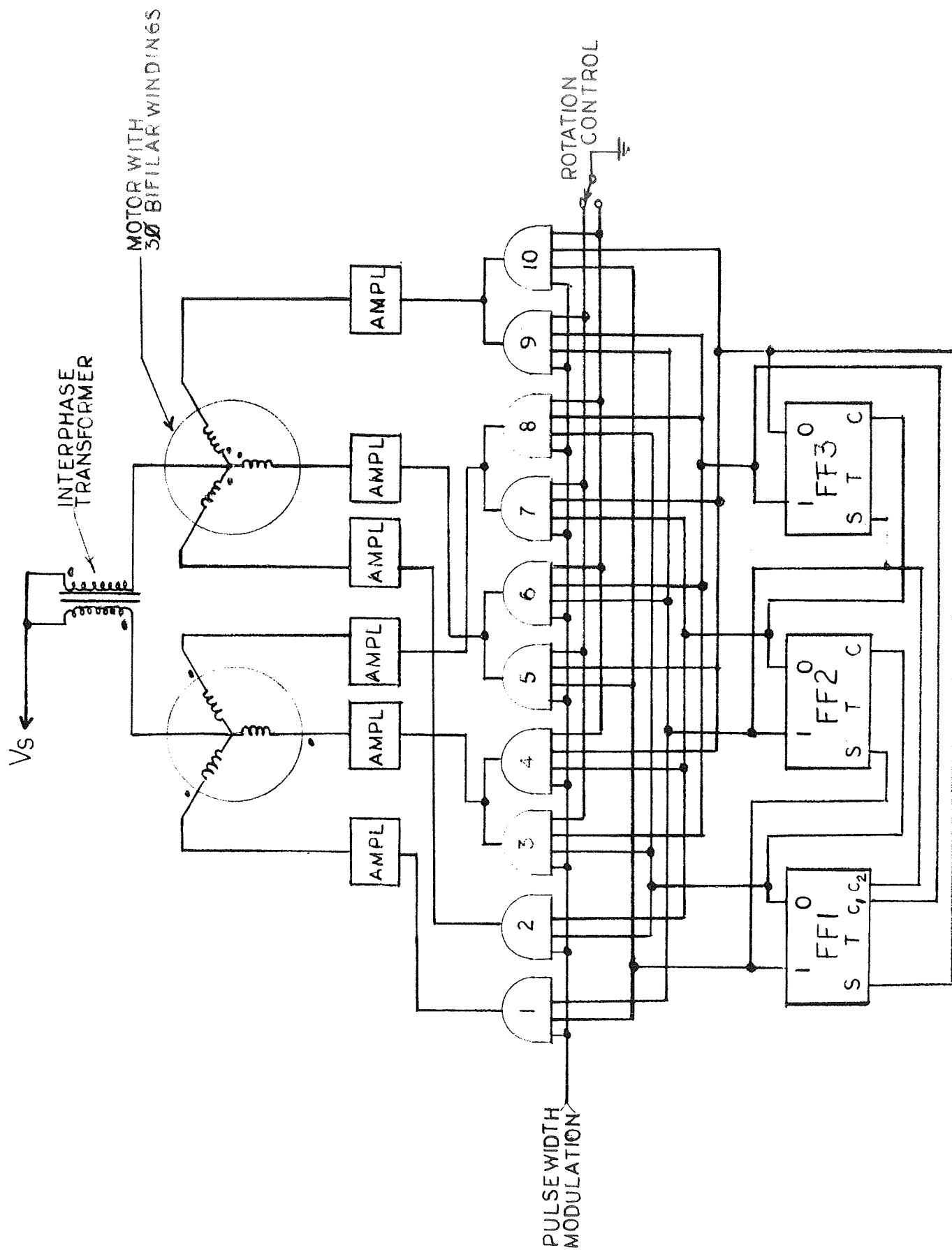


FIGURE 4. SIX PHASE HALF WAVE QUASI-SQUARE WAVE INVERTER USING RING COUNTER AND GATING CIRCUIT.

The equations for the six waveforms shown in Figure 3 are as follows:

$$A1 = FF1 \cdot FF2$$

$$B1 = \overline{FF1} \cdot FF3$$

$$C1 = \overline{FF2} \cdot \overline{FF3}$$

$$A2 = \overline{FF1} \cdot \overline{FF2}$$

$$B2 = FF1 \cdot \overline{FF3}$$

$$C2 = FF2 \cdot FF3$$

The NAND gates of the three phase quasi-square wave circuit shown on Figure 2 require three inputs per gate. The NAND gates of the six phase half wave quasi-square wave circuit shown on Figure 4 require four inputs per gate. This difference in NAND gate input requirements results in one more integrated circuit chip being necessary for the circuit on Figure 4 than is required for the circuit on Figure 2.

### 3. Current Limiting.

There are several methods of current limiting that may be used for inverter-motor systems. Two methods of current limiting are considered here. The first method, pulse width current control, is discussed in detail in this report as this was determined to be the method most compatible with high power applications. The other method of current limiting, current limiting power supply, which is more compatible with low power requirements is discussed briefly in connection with system test results. Test data of the current limiting power supply method are presented for comparison purposes.

Pulse width current limiting is achieved by gating the drive voltages to the output transistor. Several gating methods were considered. One method uses a pulse width gate that is a multiple of the input frequency.

Figure 5 shows the generation of the three phase signals and the effect of using a  $6f$  pulse-width modulating frequency. Figures 6, 7, and 8 show the variations of harmonic content versus pulse-width modulation as the modulation varies from zero to 100% for a modulation frequency of  $6f$ ,  $12f$ , and  $24f$ . The  $6f$  modulation results in two pulses per  $180^\circ$  for any one line-to-line voltage waveform.

Equations for the harmonic content of the three waveforms considered here are as follows:

$$e_n = \frac{8V}{n\pi} (\sin n \lambda) (\sin n 60^\circ), \quad 0 < \lambda \leq 30^\circ \quad (6f)$$

$$e_n = \frac{8V}{n\pi} (\sin n \lambda) (\sin n 45^\circ + \sin n 75^\circ), \\ 0 < \lambda \leq 15^\circ \quad (12f)$$

$$e_n = \frac{8V}{n\pi} (\sin n \lambda) (\sin n 37.5^\circ + \sin n 52.5^\circ \\ + \sin n 67.5^\circ + \sin n 82.5^\circ), \quad 0 < \lambda \leq 7.5^\circ \quad (24f)$$

The curves on Figures 6, 7, and 8 and Table I indicate that the harmonic content of the waveforms approximately vary with pulse width ( $\lambda$ ) until the specific harmonic being considered approaches the modulating frequency. Therefore, the modulating frequency should be as high as possible (consistent with switching capabilities of the inverter) to minimize any increase in motor losses. The inductance of the motor functions to reduce the higher frequency current.

If a motor is to be operated, for example, at a ten-to-one speed ratio by varying the input frequency, motor inductance at lower speeds will not reduce the effect of the harmonics and poorer performance than predicted will be expected.

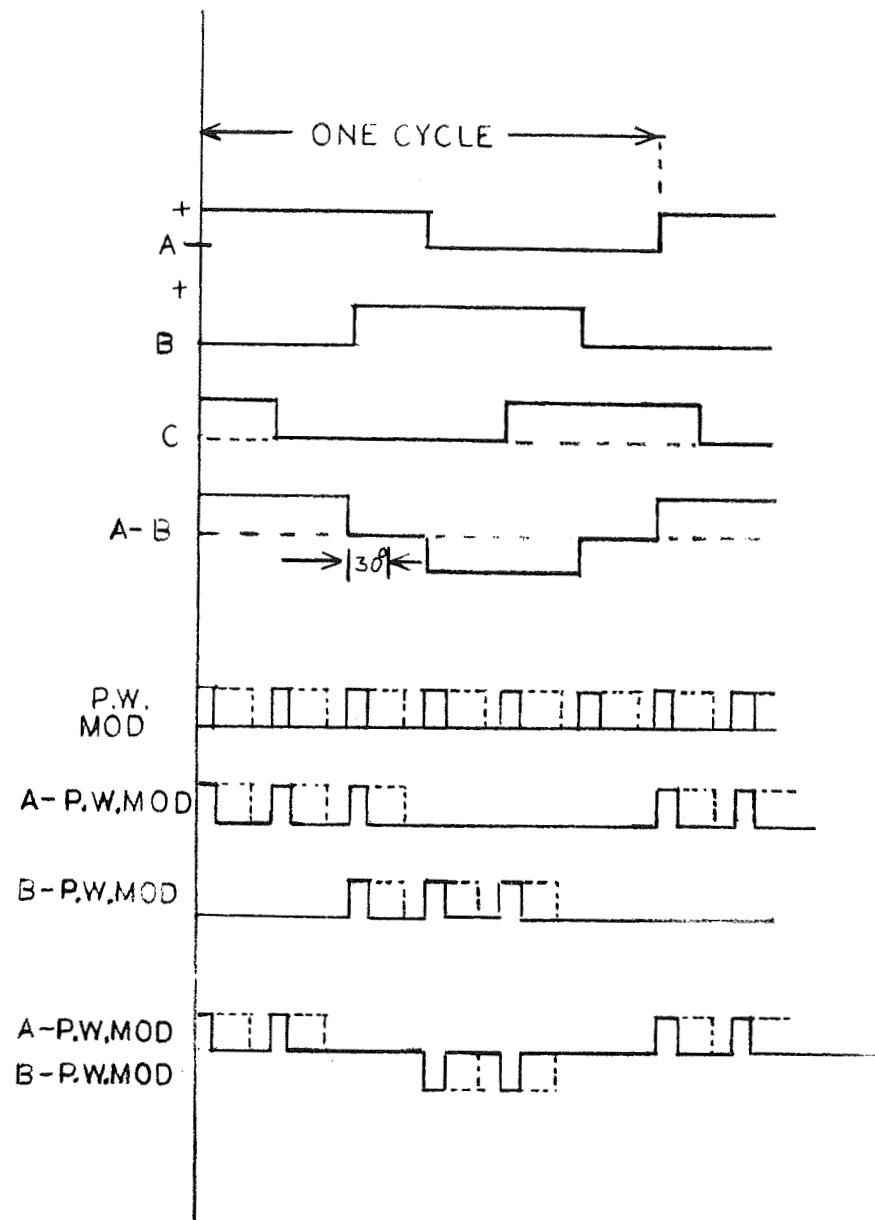


FIGURE 5. GENERATION OF PULSE WIDTH MODULATED WAVEFORM FOR CURRENT LIMITING.

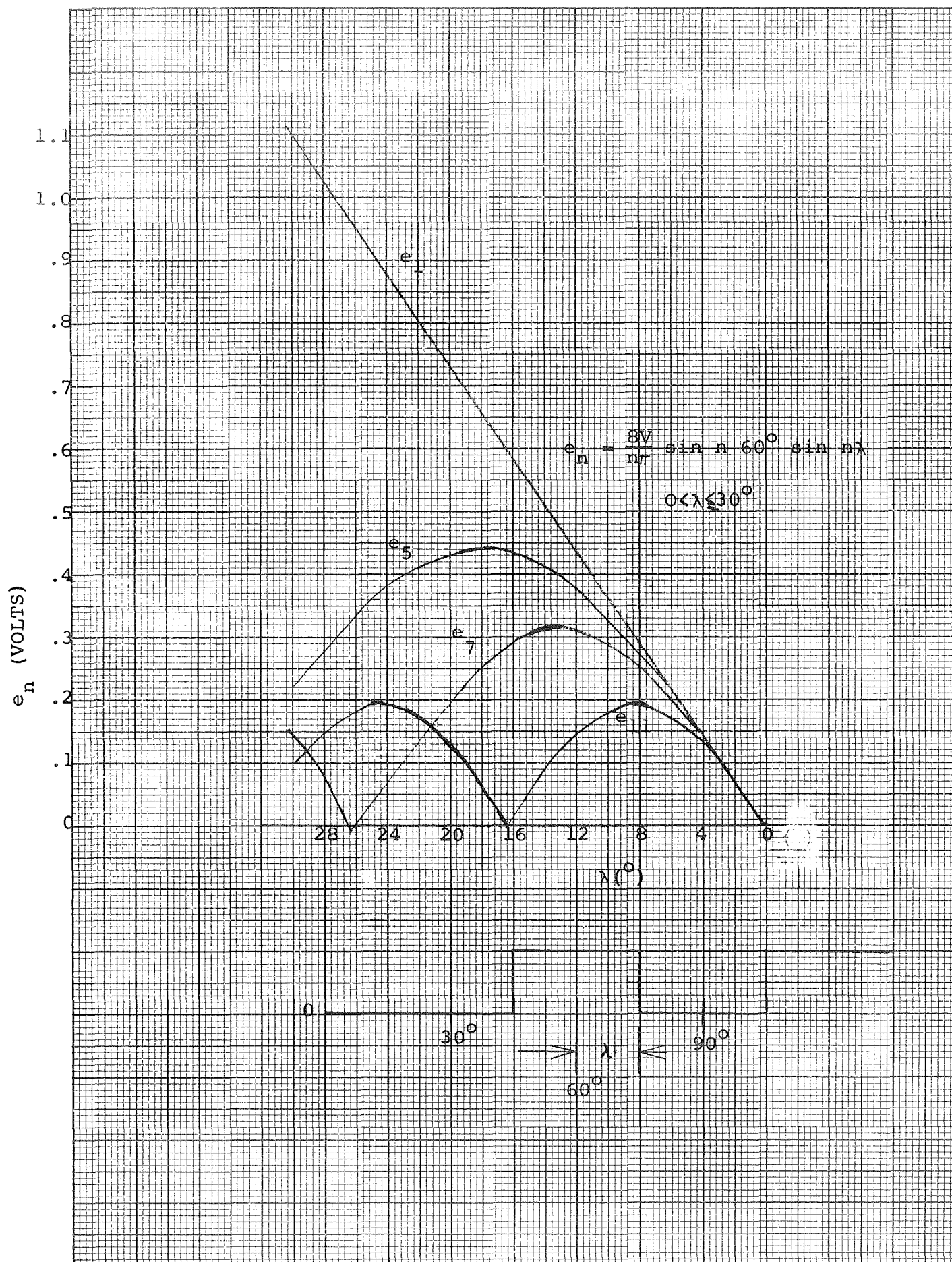


FIGURE 6. WAVESHAPE OF  $e_n$  WITH  $6f_0$  PULSE WIDTH.

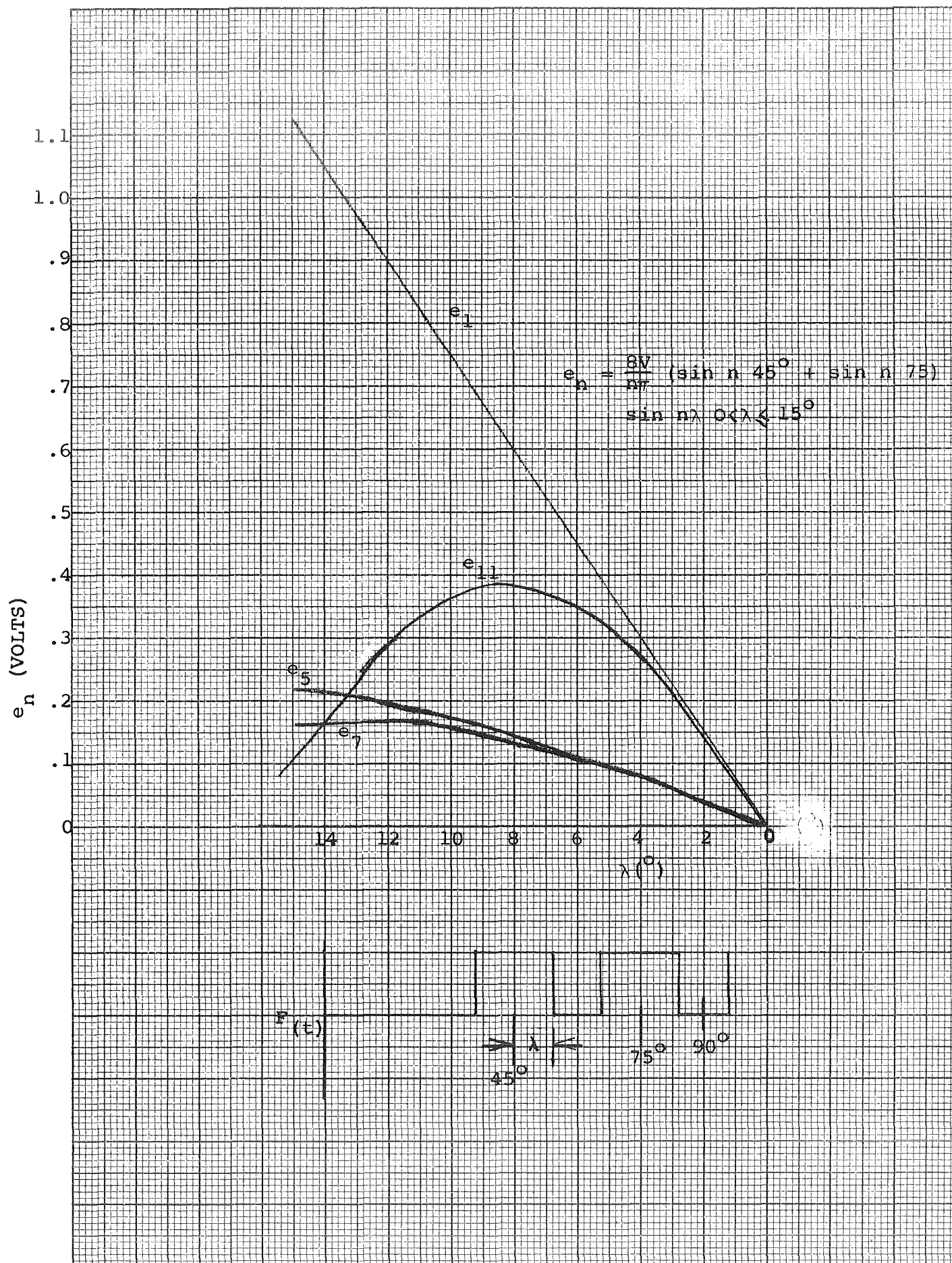


FIGURE 7. WAVESHAPE OF  $e_n$  WITH  $12f_0$  PULSE WIDTH

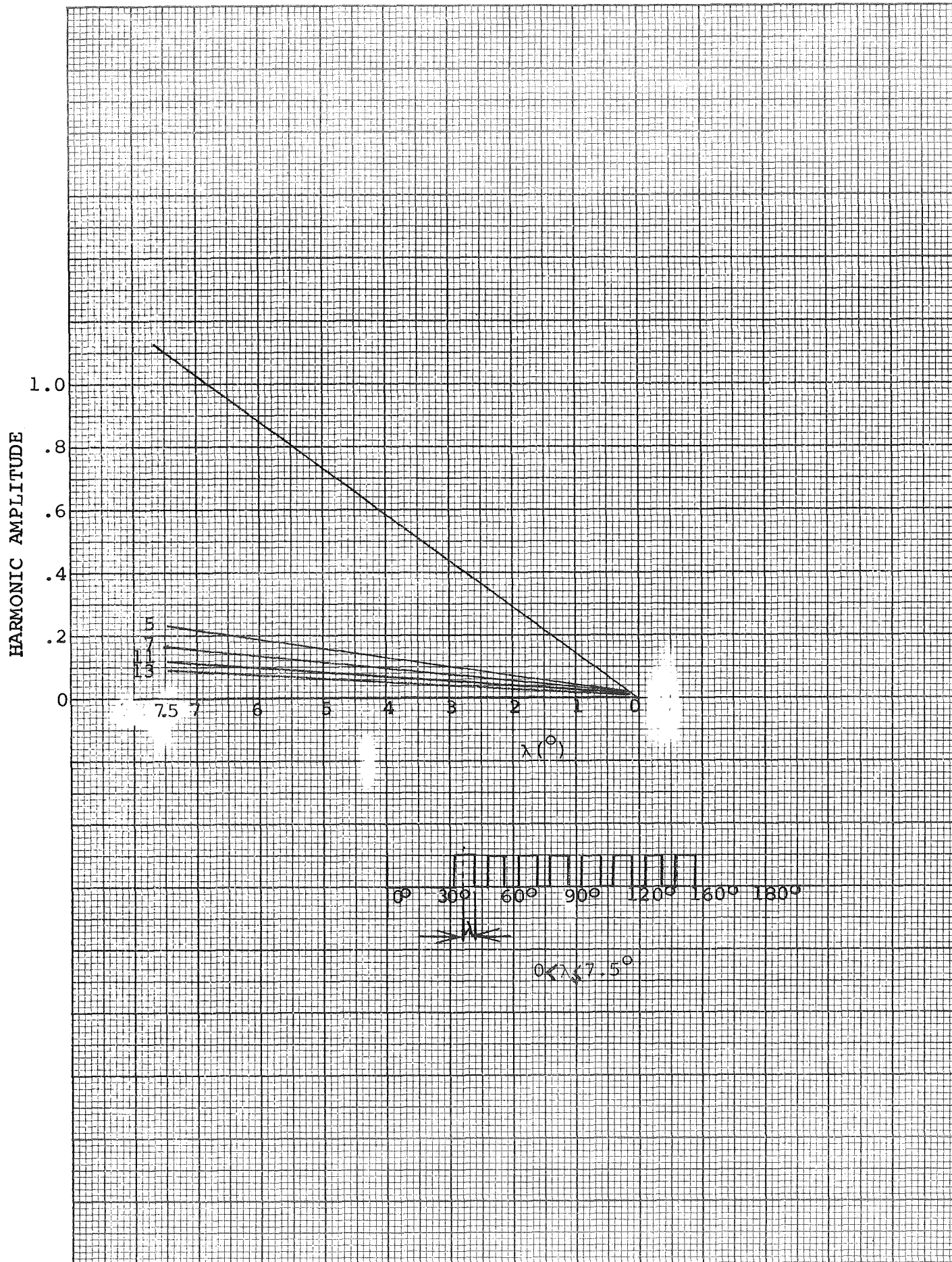


FIGURE 8. WAVESHAPE OF  $e_n$  WITH  $24f_0$  PULSE WIDTH

PULSE WIDTH (°)	% HARMONIC CONTENT FOR PULSE WIDTH CURRENT LIMITING (FIG. 6)								
	5	7	11	13	17	19	23	25	29
2	-99.5	+99.0	-97.6	96.6	-94.3	+93.0	-89.6	87.8	-83.8
6	-95.7	+91.5	-79.5	72.0	-55.1	46.0	-27.8	19.1	- 3.5
10	-88.2	77.3	-49.2	33.9	- 5.9	- 5.3	19.2	-21.7	18.7
14	-77.7	58.5	-16.5	- 1.1	+20.6	-21.7	11.1	- 2.9	-10.3
18	-64.7	37.4	+ 9.1	-20.1	15.4	- 5.3	-11.4	12.9	- 3.5
22	-50.2	16.7	21.4	-19.7	- 3.8	11.9	- 6.5	- 1.85	9.1
26	-35.0	- 1.1	20.0	- 6.6	-13.3	8.6	8.4	- 8.6	- 4.4
30	-20.0	-14.29	9.09	7.69	- 5.88	- 4.26	4.35	4.0	- 3.45

PULSE WIDTH (°)	% HARMONIC CONTENT FOR PULSE WIDTH CURRENT LIMITING (FIG. 7)								
	5	7	11	13	17	19	23	25	29
1	-26.8	-26.7	99.4	-99.2	26.4	26.3	-97.3	96.9	-25.7
3	-26.5	-26.2	94.6	-92.5	23.4	22.6	-77.6	73.8	-17.6
5	-26.0	-25.2	85.4	-80.0	18.0	16.1	-45.2	37.6	- 6.1
7	-25.2	-23.7	72.7	-63.1	11.3	8.5	-11.6	+28.1	+ 3.0
9	-24.2	-21.8	57.4	-43.8	4.57	1.4	+12.6	-18.1	5.8
11	-23.0	-19.6	40.8	-24.3	- 1.0	- 3.6	21.8	-20.9	3.2
13	-21.6	-17.0	24.3	- 6.5	- 4.6	- 5.8	16.9	-10.2	- 1.2
15	-20.0	-14.29	9.09	+ 7.69	- 5.88	- 5.26	4.35	+ 4.0	- 3.45

PULSE WIDTH (°)	% HARMONIC CONTENT FOR PULSE WIDTH CURRENT LIMITING (FIG. 8)								
	5	7	11	13	17	19	23	25	29
.5	21.4	-16.4	13.2	13.1	-16.4	-21.3	99.3	-99.2	21.2
1.5	21.4	-16.4	13.0	12.9	-15.9	-20.6	94.1	-93.0	19.4
2.5	21.3	-16.2	12.7	12.5	-15.0	-19.1	84.1	-81.3	16.2
3.5	21.1	-16.0	12.2	11.8	-13.7	-17.0	70.2	-65.5	11.9
4.5	20.9	-15.7	11.6	11.0	-12.0	-14.3	53.9	-47.1	7.2
5.5	20.7	-15.3	10.9	10.0	-10.0	-11.4	36.5	-28.2	2.7
6.5	20.4	-14.8	10.0	8.9	- 8.0	- 8.3	19.5	-10.6	- 1.0
7.5	20.0	-14.29	9.09	7.69	- 5.88	- 5.26	4.35	4.0	- 3.45

TABLE I. RELATIVE HARMONIC CONTENT AS A FUNCTION OF PULSE WIDTH.

The effect of the harmonics can be overcome by maintaining the pulsing at a high frequency. This pulsing frequency will be in the area of

12 X  $f_o$  when the input frequency is 400 Hz, and near 120 X  $f_o$  when the input frequency is 40 Hz.

Fourier Analysis of the 12f pulse width modulated quasi-square waveshape: (The waveform is half wave and has axis symmetry.)

$$e(t) = \frac{4V}{n\pi} \left[ \int_{45 - \lambda}^{45 + \lambda} \sin nx dx + \int_{75 - \lambda}^{75 + \lambda} \sin nx dx \right] \quad (1)$$

Integrating the above formula:

$$e(t) = \frac{-4V}{n\pi} \left[ \cos n(45 + \lambda) - \cos n(45 - \lambda) + \cos n(75 + \lambda) - \cos n(75 - \lambda) \right] \quad (2)$$

By using the identity  $\cos(x \pm y) = \cos x \cos y \mp \sin x \sin y$ , equation (2) reduces to:

$$e(t) = \frac{8V}{n\pi} (\sin n 45^\circ \sin n \lambda + \sin n 75^\circ \sin n \lambda) \quad (3)$$

$$\text{or } e(t) = \frac{8V}{n\pi} (\sin n \lambda) (\sin n 45^\circ + \sin n 75^\circ),$$

$n$  = order of the harmonic, 1, 3, 5 etc.

$$\text{Therefore: } e_1 = \frac{8V}{\pi} (\sin \lambda) (.7071 + .9659) =$$

$$4.26V \sin \lambda, 0 < \lambda \leq 15^\circ$$

$$e_3 = 0$$

$$e_5 = 0.228 \sin 5\lambda$$

No detailed analysis was made for this condition but test results indicate that the best performance is obtained at low frequency. Torque-speed curves do not indicate any anomalies as a result of not having the pulse width frequency synchronized to the motor line frequency.

The current limiting function of the Inverter circuit shown in Appendix I (Sheet 2 of 2) generates a waveshape corresponding to the pulse width modulated waveforms shown on Figure 5, through the following sequences.

When a pulse is applied to the  $C_D$  terminal of bistable flipflop Z102, the output of Z102 is high and the three phase signals are applied to the inverter. The same pulse that sets Z102 also sets the voltage across C104 to zero. This is accomplished by clamp transistor Q130. The voltage across C104 will then rise until unijunction transistor Q128 is triggered and the resulting pulse is used to flip Z102 off. (Figure 9 shows the pulse timing waveforms.) The charging rate of C104 is controlled by differential amplifiers Q125 and Q126, which drive current source Q127. Input current is monitored by operational amplifier Z101, and a portion of the output is used to control the differential amplifier. Low pass filter R133 and C103 is used to cause the current limiting circuit to respond to the average current rather than responding to peak pulses.

This current limiting circuit includes a provision to vary the current limiting as a function of motor speed. This is accomplished by feeding the speed sensor voltage to the input of Z101 through R129.

Additional flexibility is obtained by the use of an auxiliary oscillator (Q129, and switch S102), thereby permitting tests to be made with the current control pulses as a multiple of the oscillator frequency or at a comparatively high frequency not synchronized to the AC drive power.

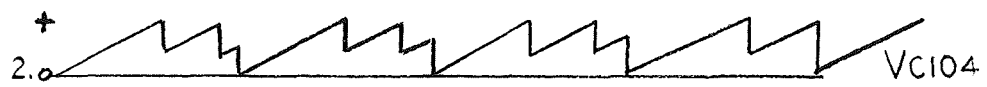


FIGURE 9. PULSE TIMING WAVEFORMS

#### 4. Slip Detector and Oscillator.

The slip detector circuit shown in the Inverter Schematic, Appendix I, compares the motor shaft speed with the inverter oscillator frequency. In normal use, this circuit is arranged to measure the shaft speed and subsequently control the oscillator so that the inverter will drive the motor at a predetermined constant slip.

The shaft speed is electrically measured and shaped by a Schmitt trigger which actuates a Fairchild 9601 monostable multi-vibrator. This circuit produces 18 pulses per shaft revolution. The output of the multi-vibrator drives current switch Q4. The output of Q4 is integrated by resistor R12 and Capacitor C2. The Fairchild 709 operational amplifier, Z2, is arranged as a unity gain amplifier. The output of Z2 is a negative going voltage which is proportional to motor speed, and operates in conjunction with a similar circuit driven by the oscillator. The RPM analogue voltage is used in obtaining torque-speed curves and when a variation of current-versus-speed control is desired.

The pulses controlling the ring-counter (which in turn controls the output frequency) are generated by uni-junction transistor Q9. Pulse frequency is determined by capacitor C10 and resistor R42, which are connected in parallel with current source Q8. When the base of Q8 is connected to a +10 volt source, resistor R42 and capacitor C10 control the oscillator frequency.

Normally Q8 is driven by differential amplifier Q6 and Q7, with resistor R42 adjusted to maximum resistance. The output of Q9 is shaped by a NAND gate and divided by four by two binarys, Z6 and Z7. Binarys Z6 and Z7 permit a current control signal to be generated.

The current control signal is 24 times the output frequency which results in the pulse width current limiting method. The output of flipflop Z7 is used

in the slip control circuit and from there the flip flop output goes to the ring counter for 3 phase generation through NAND gates. These NAND gates function to alleviate a noise problem that caused false triggering in the count down circuits.

A DC voltage, proportional to the oscillator frequency, is generated by the "one shot" action of Z3, Q5 and C6. This DC voltage is compared to the "RPM" voltage from Z2 and the sum is amplified by operational amplifier Z3. Note the voltage from C6 is positive and the voltage from Z2 is negative, therefore the output of Z3 is a function of the difference between the oscillator and the motor speed frequency. Z3, arranged as an integrator to minimize fluctuation, has a gain which is set by the ratio of R22 to R20 and R21. This voltage is applied to differential amplifier Q6 and Q7 and the circuit functions to maintain constant voltage at the base of Q6.

The output of Z2 is approximately 0.82 volts with a pulse rate of 2400 pulses per second. This pulse rate is equivalent to a motor speed of 8000RPM, which is the nominal no load speed. The gain of operation amplifier Z4 can be computed from the relationship  $I_{R20} + I_{R21} = I_{R22}$  (R20 = R21 = 10.5K, R22 = 110K). Therefore, the gain of the operational amplifier is

$$\frac{E_0}{E_1 + E_2} = \frac{R22}{R20} = \frac{110}{10.5} = 10.5.$$

Since  $E_2$  is inverted by Z2 the output represents the difference between the oscillator and motor frequency and the  $\Delta E_0$  for a one pulse per second difference is  $10.5 \times \frac{.82}{2400}$  volts or 3.6 mv. The measured gain from Z4 to the emitter of Q8 is 12. R40 and R41 are 4.7K ohms so the charging current to C10 is  $\frac{3.6 \times 12}{4.7K}$  or 9.1  $\mu$ amps

and the value of C10 is 0.01 MFD. The gain of this circuit may be changed by varying the values of R36 or R40. R40 functions primarily to set an upper frequency limit.

Slip control is set by adjusting the offset of Z4 by R25. R8 controls the relative pulse width of the two monostable multi-vibrators. Therefore, by adjusting R25 and R8 the unit will drive the motor at any reasonable slip, and the absolute slip frequency can be set to increase or decrease as the motor speed increases. Motor braking will result if R25 is set for negative slip.

Calibration of this circuit is accomplished by connecting an audio oscillator to inject an audio signal at the base of Q2. The input and output frequencies are measured with a frequency counter. The frequency measured by the counter is six times the inverter output frequency as a result of a ring counter being used for three phase generation (a display of 2400 Hz is equivalent to 400 Hz at the Inverter output).

Fixed frequency operation is obtained by using switch S2 to connect the base of Q8 to +10 volts, thereby cutting off Q8 and opening the speed feedback loop. Manual frequency control is then obtained by adjusting resistor R42.

##### 5. Output Circuit.

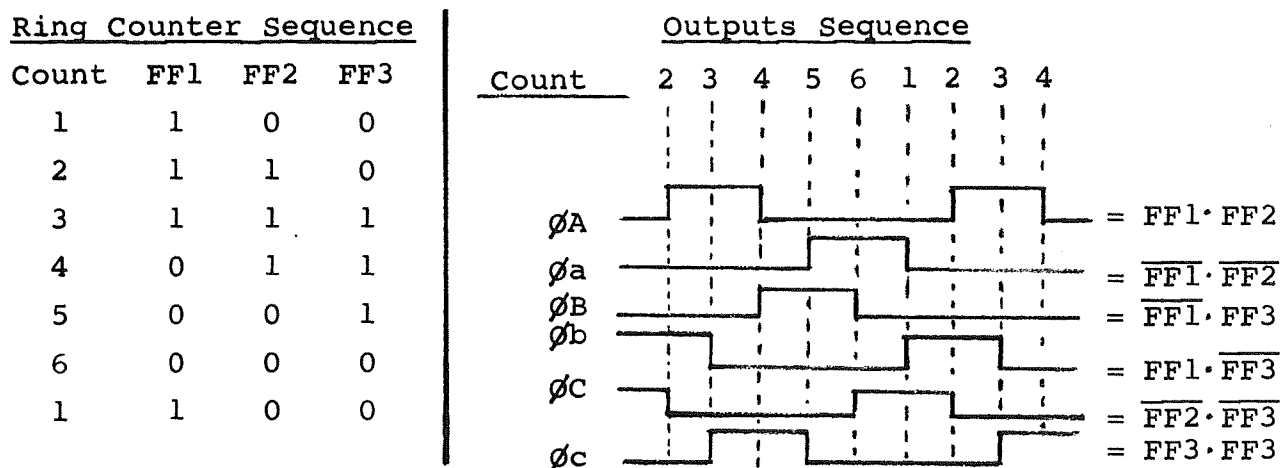
The Inverter Schematic in Appendix I shows a conventional transformerless three phase quasi-square wave inverter connected directly to the motor. This inverter is unique in that there are no driver transformers used in its design. The inverter in this configuration does not impose any low frequency limitation on system operation.

The three phase signals, generated by a "switched tailed" ring counter, pass through gates to the inverter. The gates perform two functions: (1) Rotation control, achieved by interchanging phases B and C, and (2) a pulse width current control signal, added at this point for current limiting.

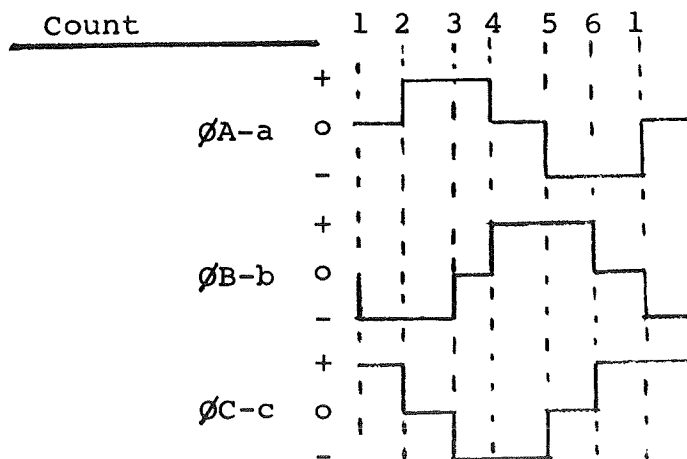
A six phase half wave inverter circuit was evaluated with quasi-square wave drive, square wave drive, and with and without interphase transformer T1.

The six phase ring-counter logic operates as follows.

(Note: The curves represent optimum operation.)



With  $\phi A$  representing the bifilar winding, the phase currents with a resistive load would be as follows:



6. Miscellaneous Circuits.

A DC to DC converter was added to furnish the isolated DC voltage which is required for the logic circuit and operational amplifiers.

#### IV. SYSTEM TEST.

##### A. Inverter Breadboard Design and Test Results.

An Inverter breadboard was constructed to evaluate inverter-motor system performance and to test the effectiveness of the constant slip concept. The schematic of the Inverter breadboard as it exists at the end of the Study Program is located in Appendix I. A block diagram of the Inverter is presented in Appendix II.

##### 1. Current Control.

##### a. Pulse Width Current Limiting. (Motor No. 1)

Inverter-motor system tests were conducted with the preliminary design of the current sensing and limiting circuit (shown on Figure 10) in the Inverter. The load motor, which is not illustrated, was adjusted to operate at approximately 4800RPM.

Input and output power was measured, the results are presented on the following table. (Inverter output approximately 450Hz.)

CURRENT SENSING AND LIMITING CIRCUIT TEST DATA

PHOTO NO.	$E_{in}$ (VDC)	$I_{in}$ (AMPS)	$P_{in}$ (WATTS)	TORQUE (OZ-IN.)	MOTOR SPEED (RPM)	$P_{out}$ (WATTS)	EFFICIENCY (%)
1	28	2	56	5.6	4810	14.1	25.2
2	28	3	84	10.0	4873	36.1	43.0
3	28	4	112	14.6	4933	53.4	47.6
4	28	5	140	18.4	4956	67.4	48.3
5	28	6	168	23.7	4980	87.5	52.2
6	28	7	196	28.2	4993	104.0	53.0
7	28	8	224	31.8	4999	112.5	52.5
8	28	9	252	37.0	5030	137.5	54.6
9	28	9.6	269	41.0	5050	153.0	57.0

Oscilloscope photographs are presented in Figures 11, 12, and 13.

The oscilloscope photographs show the waveforms of:

A. On-off pulse width ratio of voltage applied to the driver base of a transistor. B. Phase A motor input current. Photograph No. 9, Figure 13 is the waveform obtained when the current limiting was adjusted for no current limiting.

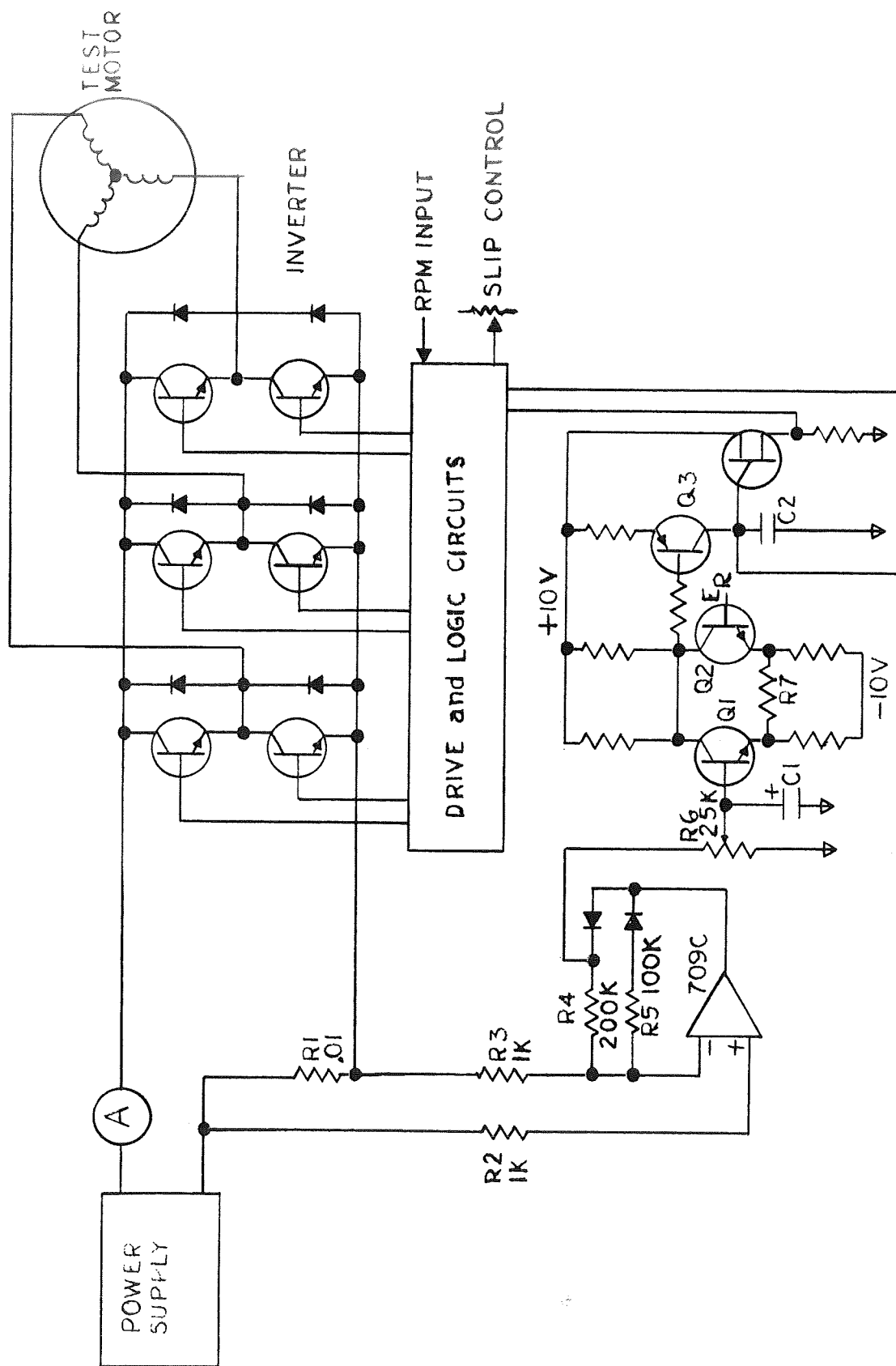


FIGURE 10. TEST SETUP WITH PULSE WIDTH CURRENT SENSING AND LIMITING CIRCUIT (PRELIMINARY DESIGN)

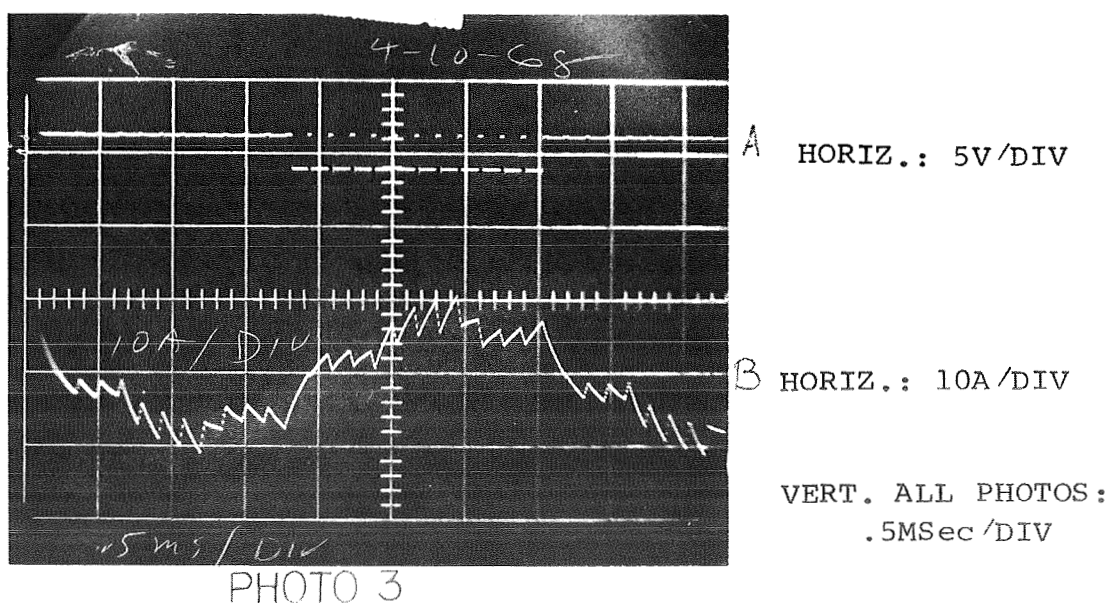
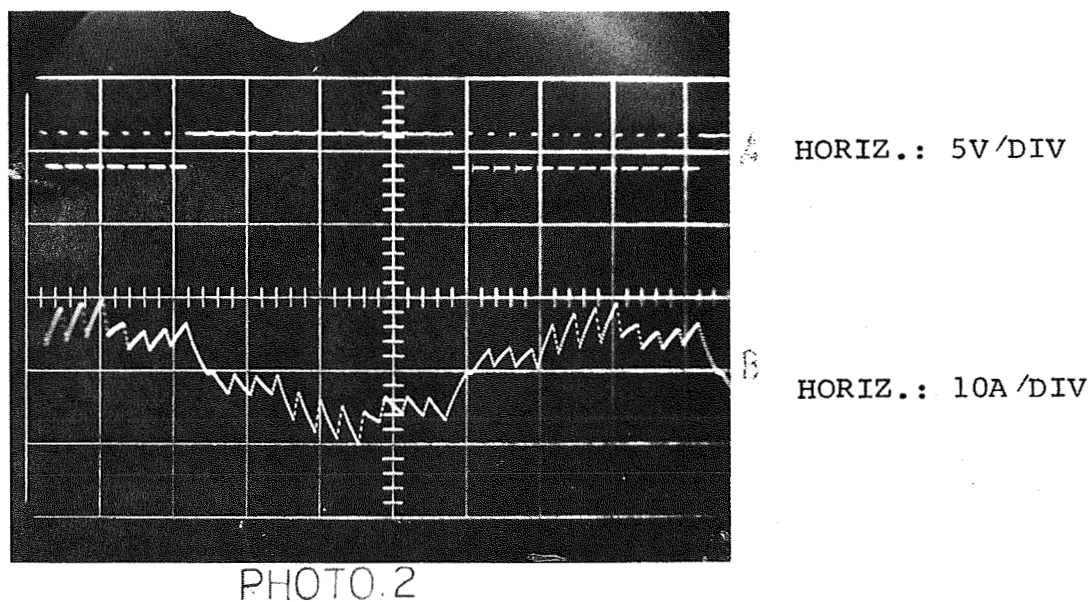
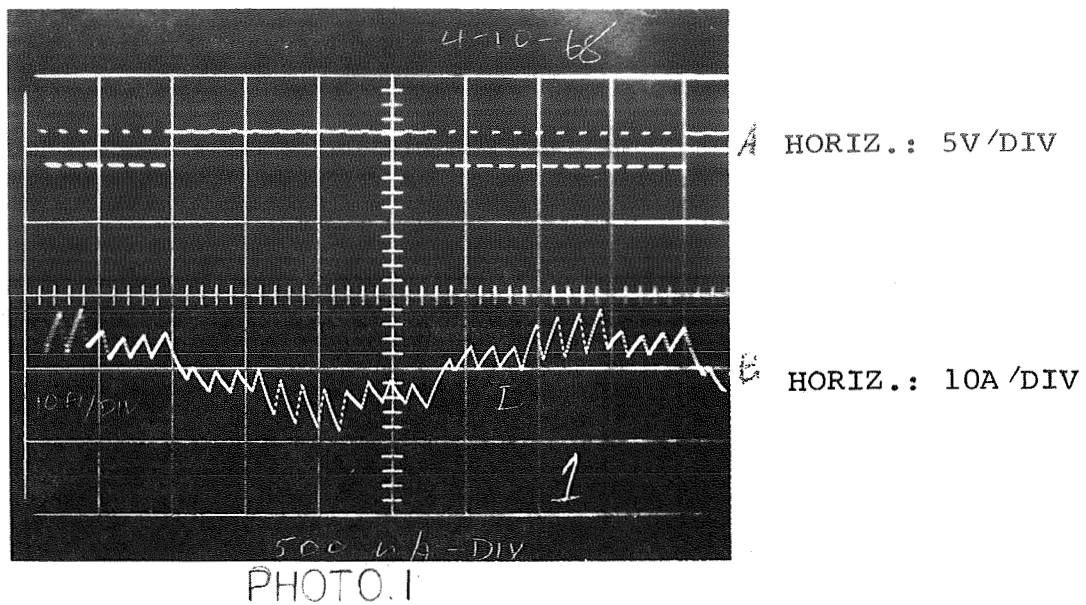
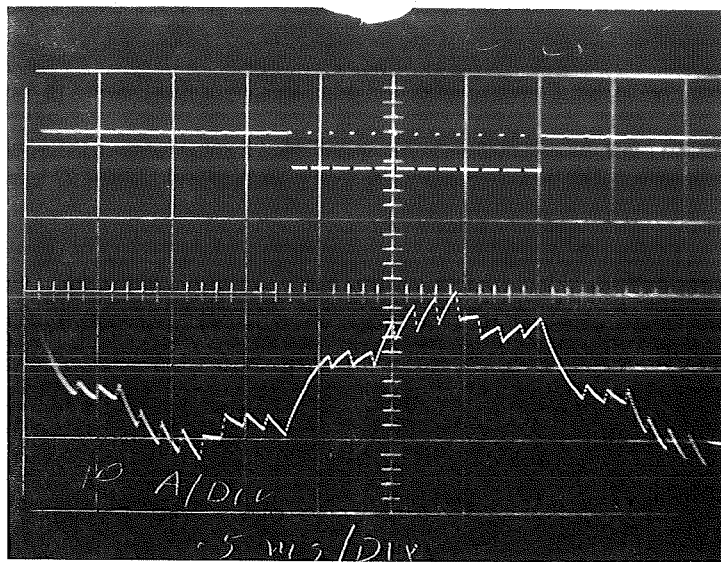


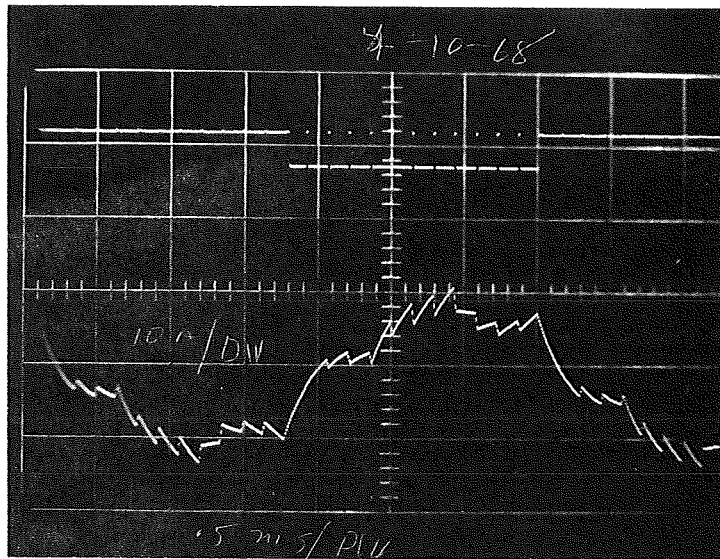
FIGURE 11. OSCILLOSCOPE PHOTOGRAPHS 1,2,3.



A HORIZ.: 5V/DIV

B HORIZ.: 10A/DIV

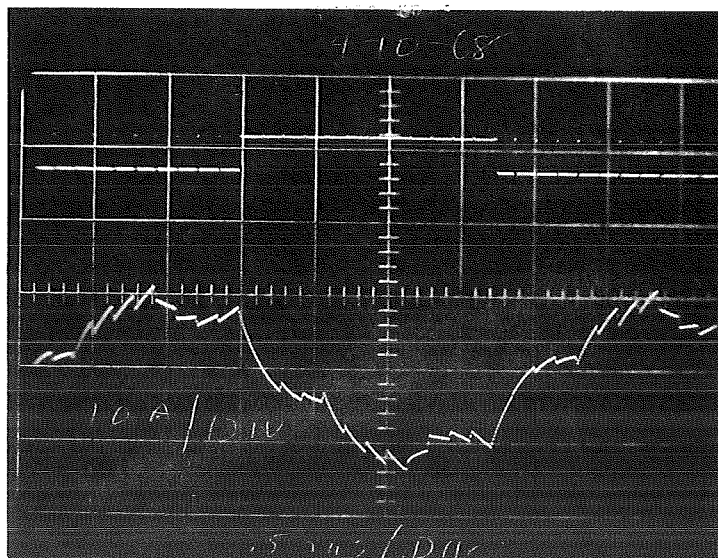
PHOTO.4



A HORIZ.: 5V/DIV

B HORIZ.: 10A/DIV

PHOTO.5



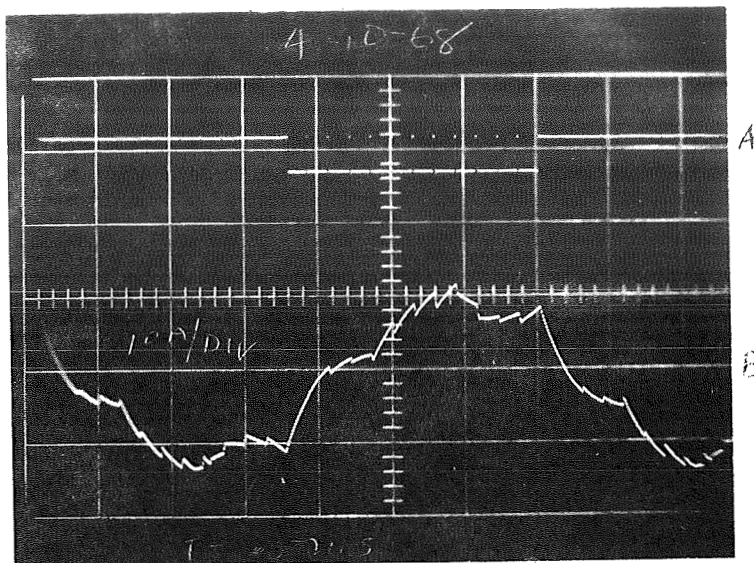
A HORIZ.: 5V/DIV

B HORIZ.: 10A/DIV

VERT.: ALL PHOTOS:  
.5MSEC/DIV

PHOTO.6

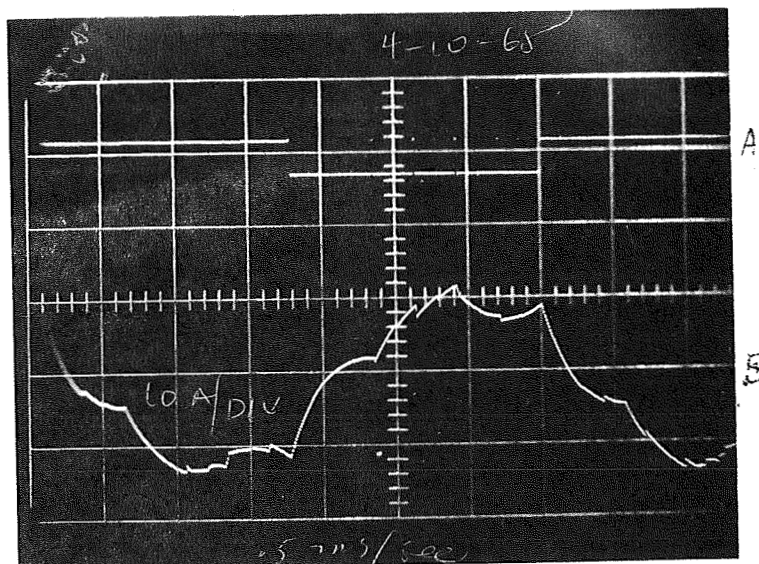
FIGURE 12. OSCILLOSCOPE PHOTOGRAPHS 4,5,6.



HORIZ.: 5V/DIV

HORIZ.: 10A/DIV

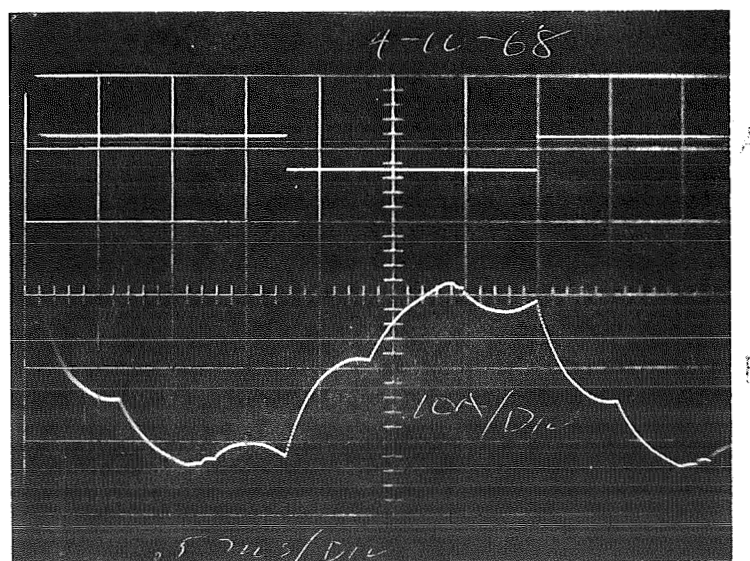
PHOTO.7



HORIZ.: 5V/DIV

HORIZ.: 10A/DIV

PHOTO.8



HORIZ.: 5V/DIV

HORIZ.: 10A/DIV

VERT. ALL PHOTOS:  
.5MSEC/DIV

PHOTO.9

FIGURE 13. OSCILLOSCOPE PHOTOGRAPHS 7,8,9.

The test setup shown on Figure 14 was used to investigate the possibility of motor operation at a constant slip. The curves on Figure 15 are defined as (A) Torque at Constant Frequency, and (B) Torque at Constant Slip. The slip was adjusted for maximum torque value. Curve (B) indicates a constant torque of 50 oz-in until the Inverter is no longer current limiting.

In a situation requiring acceleration of a mass, the available torque is considerably large, as shown on Figure 15, when the Constant Slip curve (B) is compared to the 400 Hz Constant Frequency curve, the torque increase is a 10 to 1 ratio. (Dips in the curves on Figure 15 are the result of mechanical resonances. For curves obtained at a later date the dips were eliminated by using stiffer mechanical couplings.)

The current sensing and limiting circuit shown on Figure 14 incorporates the following design modifications: The 709C operational amplifier feedback circuit was modified to make the sense voltage a function of the average Inverter input current. Previously only the positive current was sensed. The R-C filter across the input current sense circuit was also changed as input current spikes caused erratic recorder operation. Figure 14 also shows the test setup to evaluate the final current sensing and limiting circuit design. The test setup allows measurement of motor torque and input current as a function of motor speed. The curves shown on Figures 16, 17, and 18 were obtained under the following test conditions:

The slip control circuit was adjusted to produce a constant slip frequency of 25 Hz.

The input DC voltage was maintained at a constant 20 VDC.

The lock rotor torque was measured by keeping the shaft in a fixed position while power was applied.

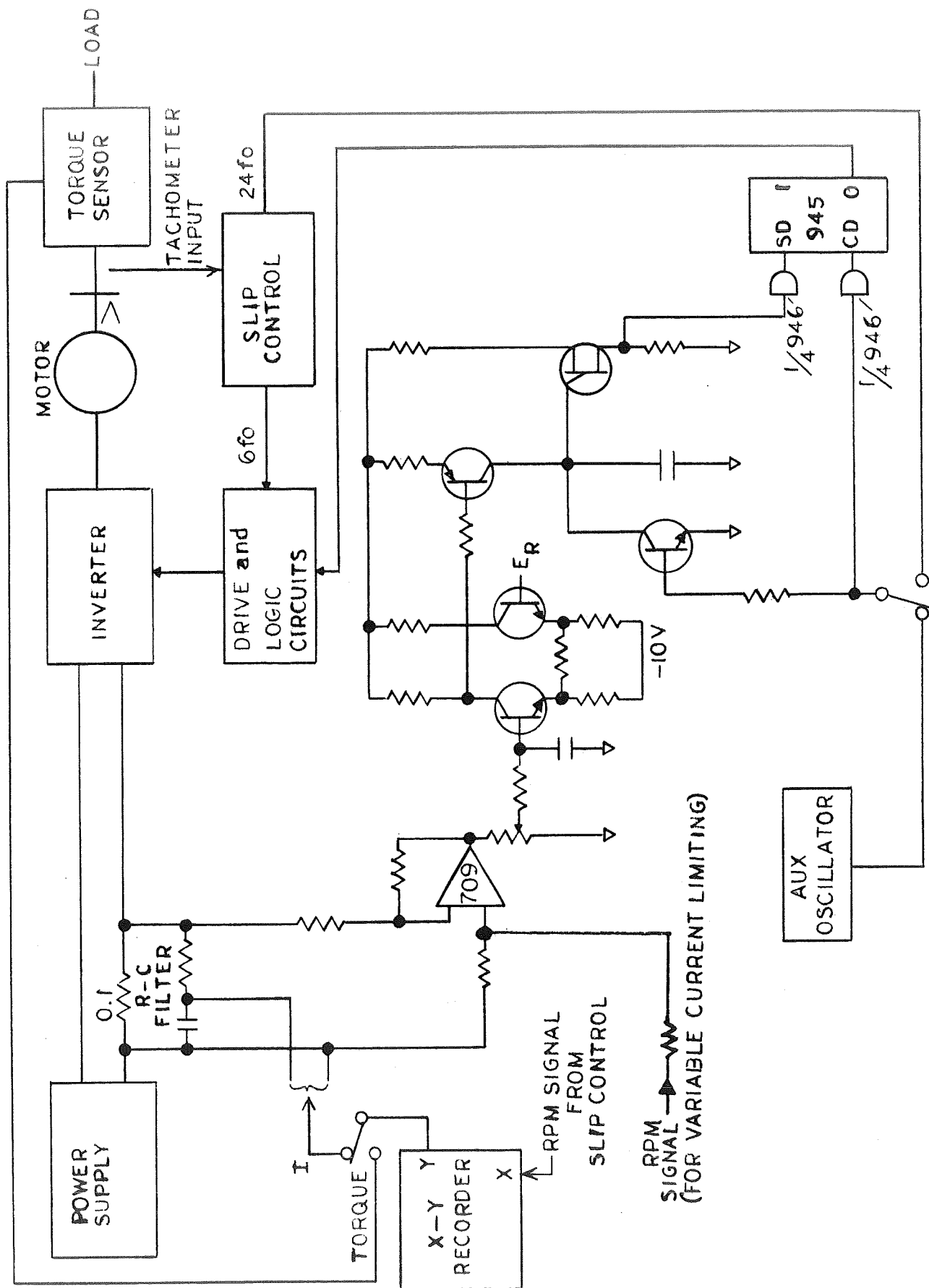


FIGURE 14. TEST SETUP WITH REVISED PULSE WIDTH CURRENT SENSING AND LIMITING CIRCUIT (FINAL DESIGN).

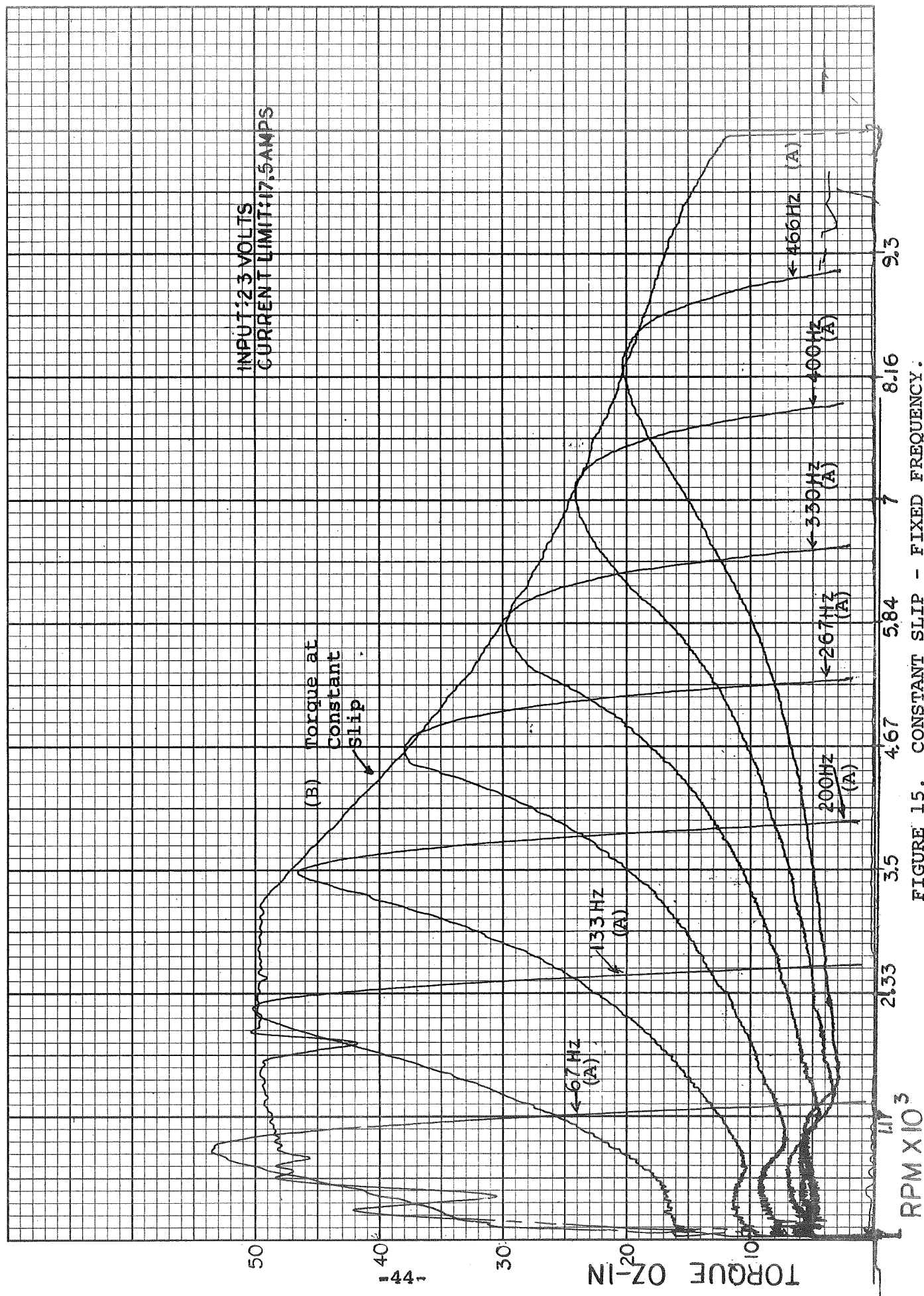
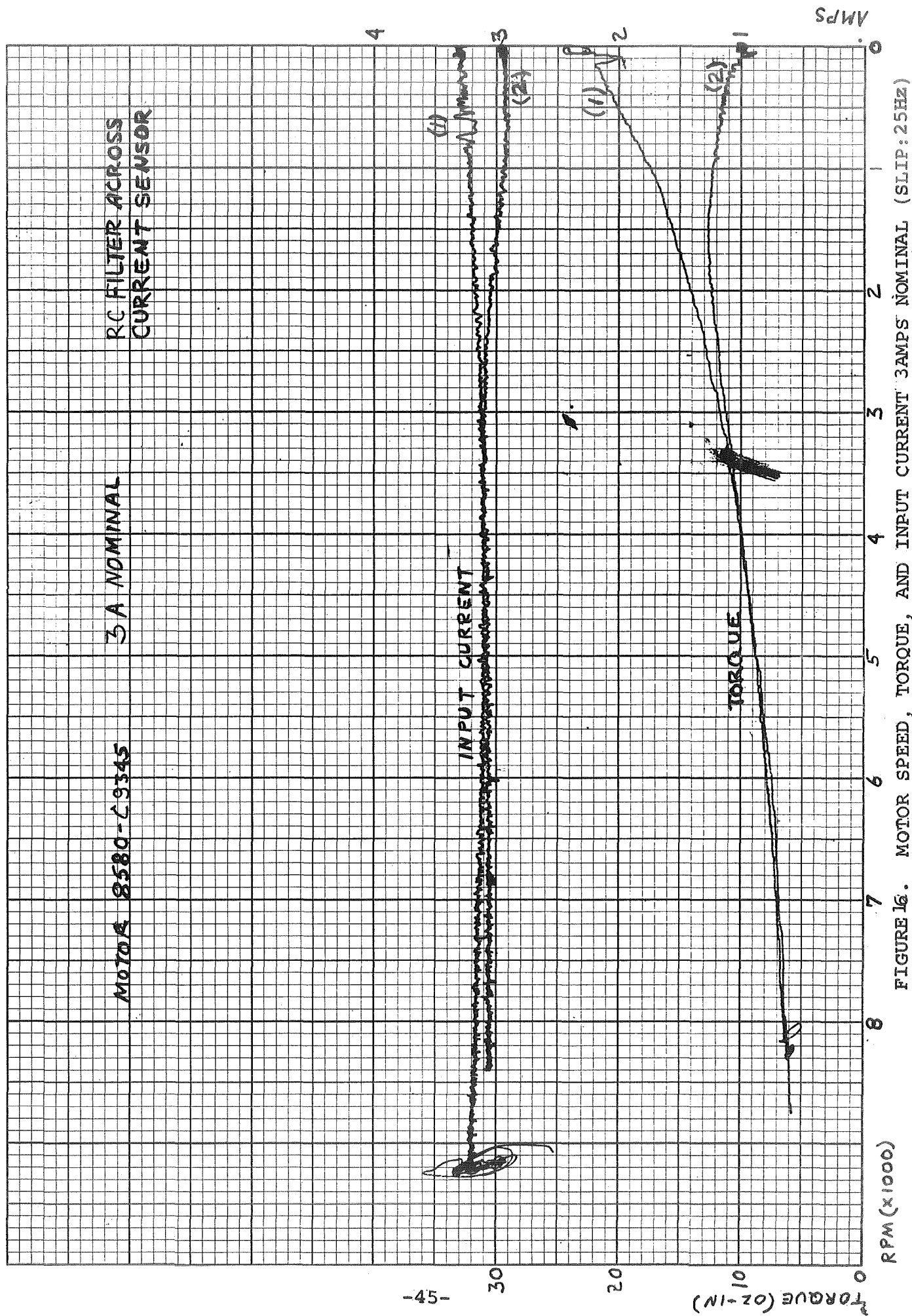
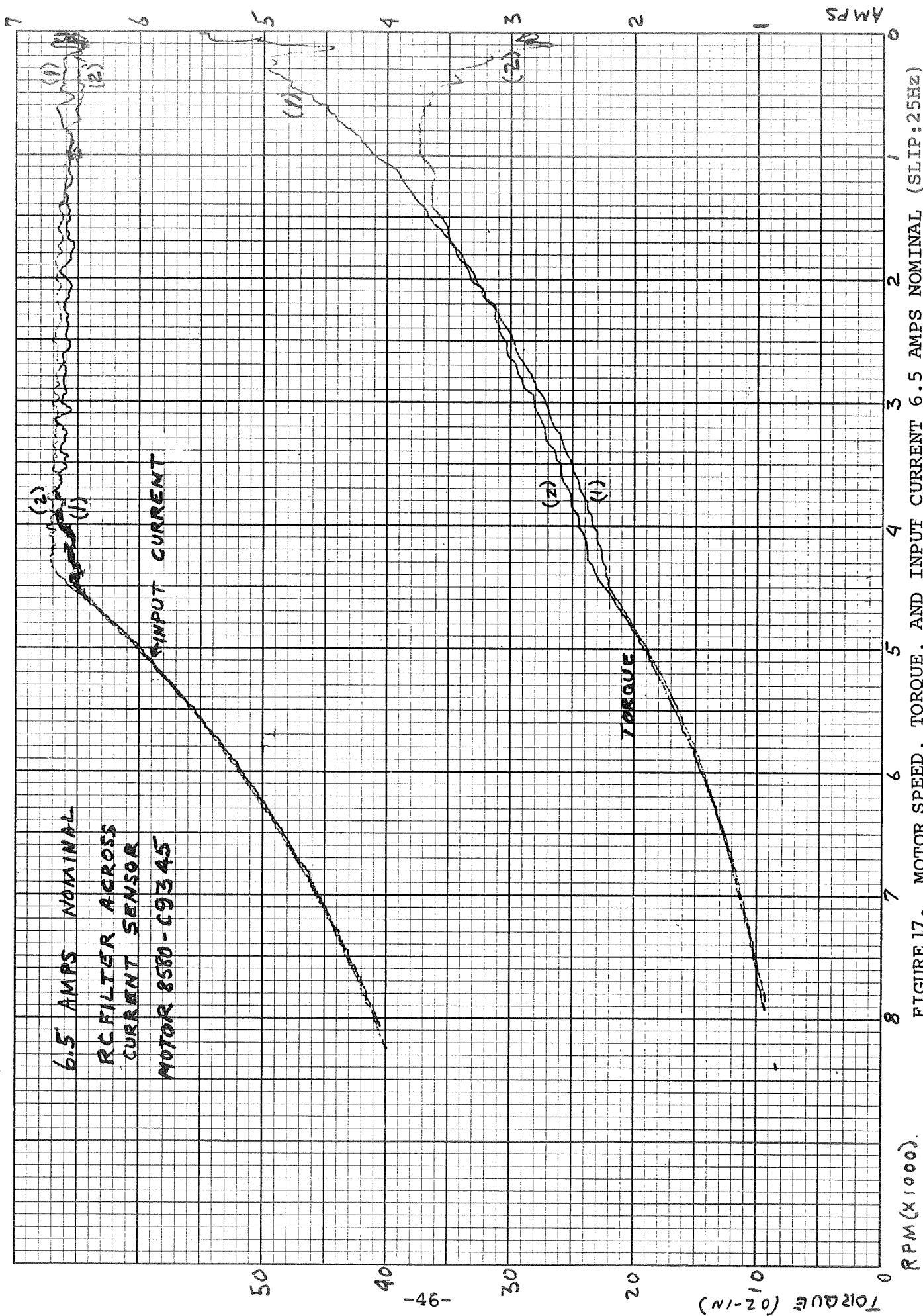


FIGURE 15. CONSTANT SLIP - FIXED FREQUENCY.





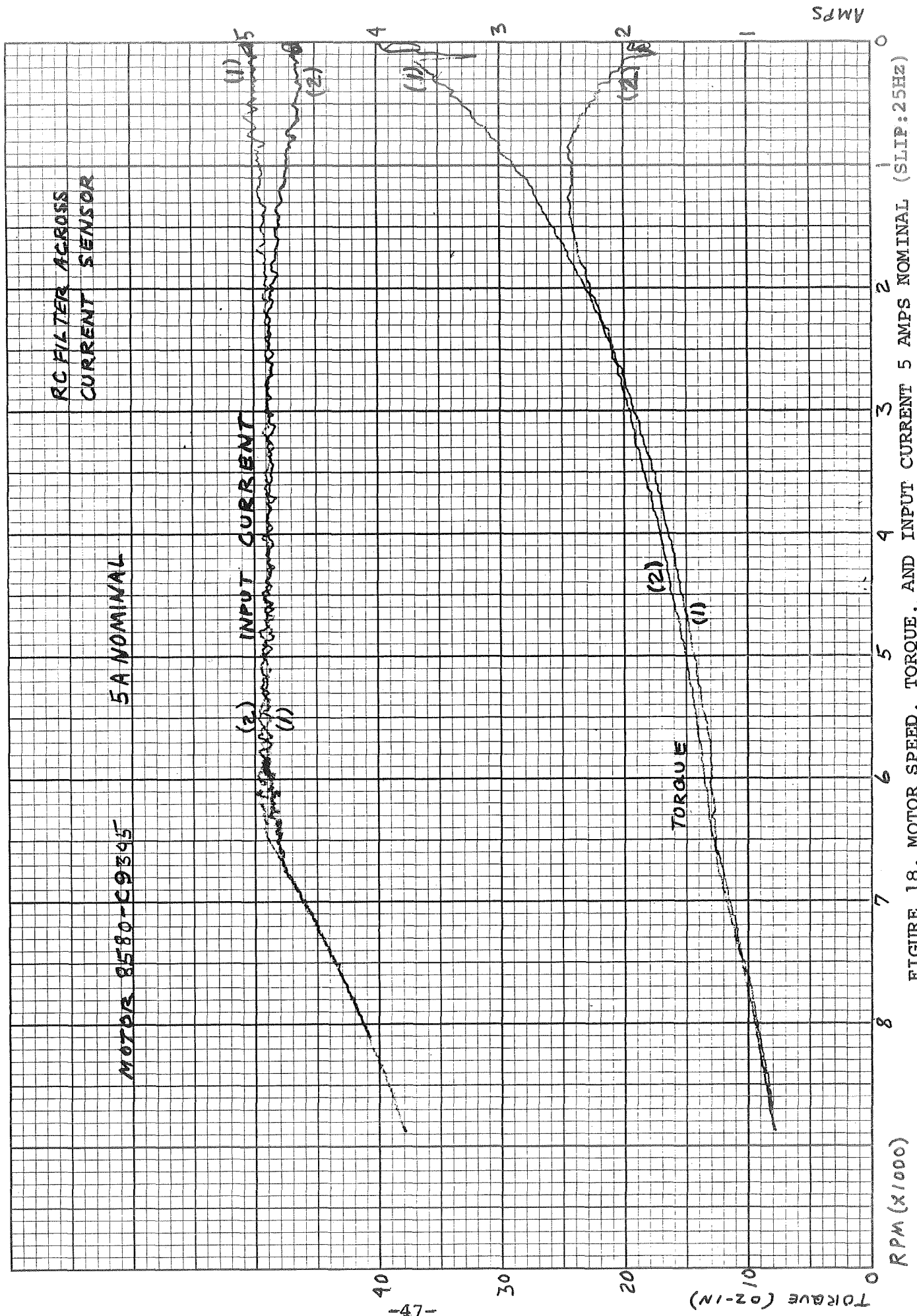


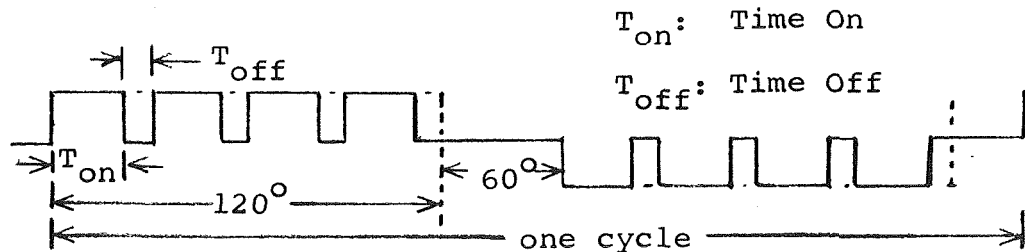
FIGURE 18. MOTOR SPEED, TORQUE, AND INPUT CURRENT 5 AMPS NOMINAL (SLIP: 25HZ)

The curves on Figures 16, 17, and 18 are read from right to left, as the slip detector output voltage representing RPM is negative with respect to ground while other voltages to the recorder are positive.

Curve 1 in each graph shows the input current and torque obtained with the free running oscillator in the circuit. Curve 2 shows input current and torque obtained when the Inverter oscillator was used. The dips that appear in the torque curves at extremely low speeds are assumed to have been caused by system time constants. The latter may have too long a duration to compensate for the rapid change in acceleration at system turn-on.

The increase in stall torque using high frequency current control, shows approximately a two-fold improvement as compared to the synchronous frequency control method.

Current control is achieved by varying the on-to-off ratio ( $T_{on}$  and  $T_{off}$ ) at a repetition rate that is faster than the fundamental frequency, as shown in the following diagram.



The on-off switching frequency can be derived from the output of the oscillator which generates the fundamental frequency, or a free-running oscillator output set to approximately 8KHz may be used.

The curves on Figures 19, 20 and 21 are initial torque-speed curves for Motor No. 1, obtained using the test setup of Figure 14. Pulse width

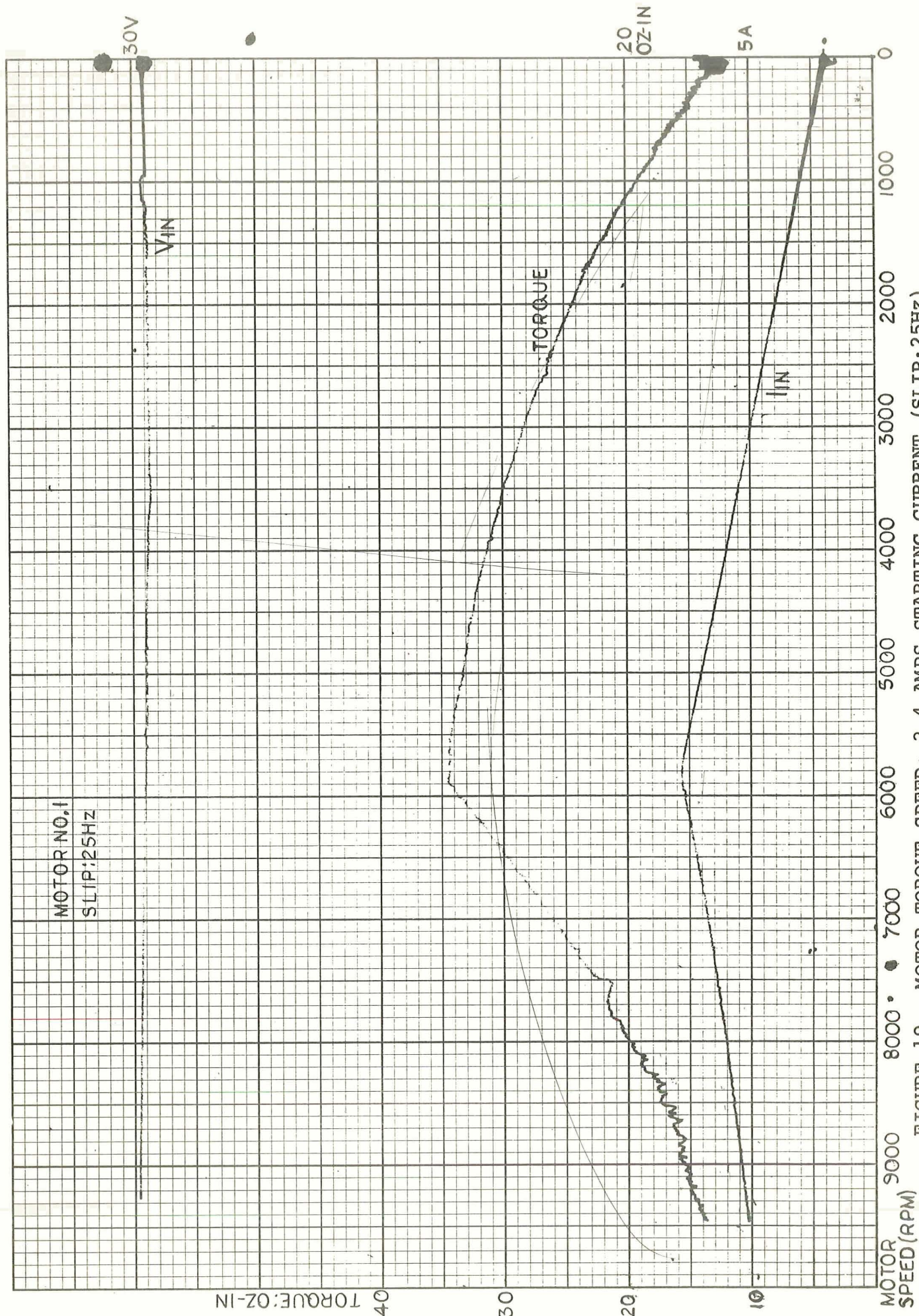


FIGURE 19. MOTOR TORQUE-SPEED: 2.4 AMPS STARTING CURRENT (SLIP: 25HZ)



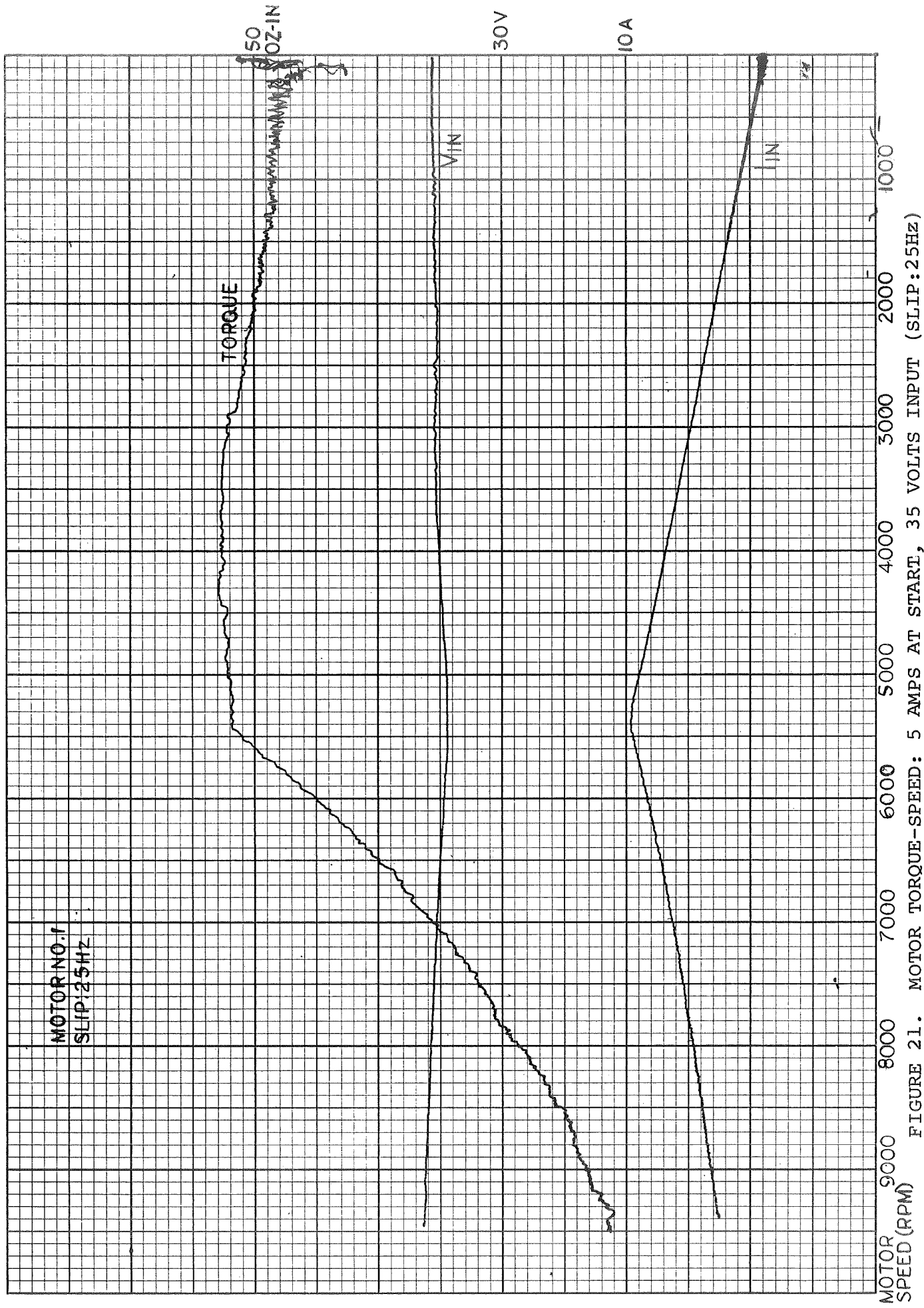


FIGURE 21. MOTOR TORQUE-SPEED: 5 AMPS AT START, 35 VOLTS INPUT (SLIP: 25Hz)

current limiting was employed, using the free running oscillator. The current limit set point was varied as a function of motor speed by adding the "RPM" signal to the input of the current sensing amplifier (709 operational amplifier). The curve on Figure 19 was obtained with an input voltage of 30 volts and a 2.4 amp starting current. The input voltage for the curve on Figure 20 was 30 volts with the current set for approximately 5 amps at motor starting. The curve on Figure 21 was obtained with a 5 amp motor starting current and 35 volts input. The slip was set at a constant of 25 Hz for each test condition. The following table presents the efficiency at various motor speeds as related to Figures 19, 20, and 21.

EFFICIENCY TABLE (SLIP = 25Hz)

MOTOR SPEED (RPM)	EFFICIENCY (%)		
	2.4 AMPS STARTING CURRENT 30 V in (FIG 19)	5 AMPS STARTING CURRENT, 30 V in (FIG 20)	5 AMPS STARTING CURRENT, 35 V in (FIG 21)
500	7.5	10.7	10.3
1000	15.9	19.0	18.7
2000	30.5	35.3	32.8
3000	42.6	47.4	44.5
4000	52.4	56.1	52.9
5000	59.5	62.6	58.8
6000	65.6	64.9	62.7
7000	67.4	68.0	63.7
8000	65.8	67.3	64.3
9000	64.1	67.3	64.4

The results of this evaluation indicate that constant acceleration torque may be obtained with variable current limiting. In addition, there is no apparent increase in efficiency at low motor speeds.

b. Current Limiting Power Supply At Various Slip Operation. (Motor No. 1)

The information presented in this section is for the purpose of comparing results of current limiting power supply operation versus the pulse width current limiting method of current control.

An inverter incorporating a current limiting power supply was breadboarded. Motor torque-speed curves shown on Figures 22, 23 and 24 were obtained using a current limiting power supply method. The following table shows motor efficiency at slip frequencies of  $8 \frac{1}{3}$ ,  $16 \frac{2}{3}$ , and  $33 \frac{1}{3}$  Hz and specific motor running speeds (RPM).

EFFICIENCY WITH CURRENT LIMITING AT APPROXIMATELY 10 AMPS.

MOTOR SPEED (RPM)	EFFICIENCY (%)		
	AT SLIP (Hz)		
	$8 \frac{1}{3}$	$16 \frac{2}{3}$	$33 \frac{1}{3}$
500	12	17	13
1000	20	28	23
2000	28	41	36
3000	42	52	45
4000	52	57	51
5000	55	60	55
6000	58	62	56
7000	56	61	58
8000	57	64	53

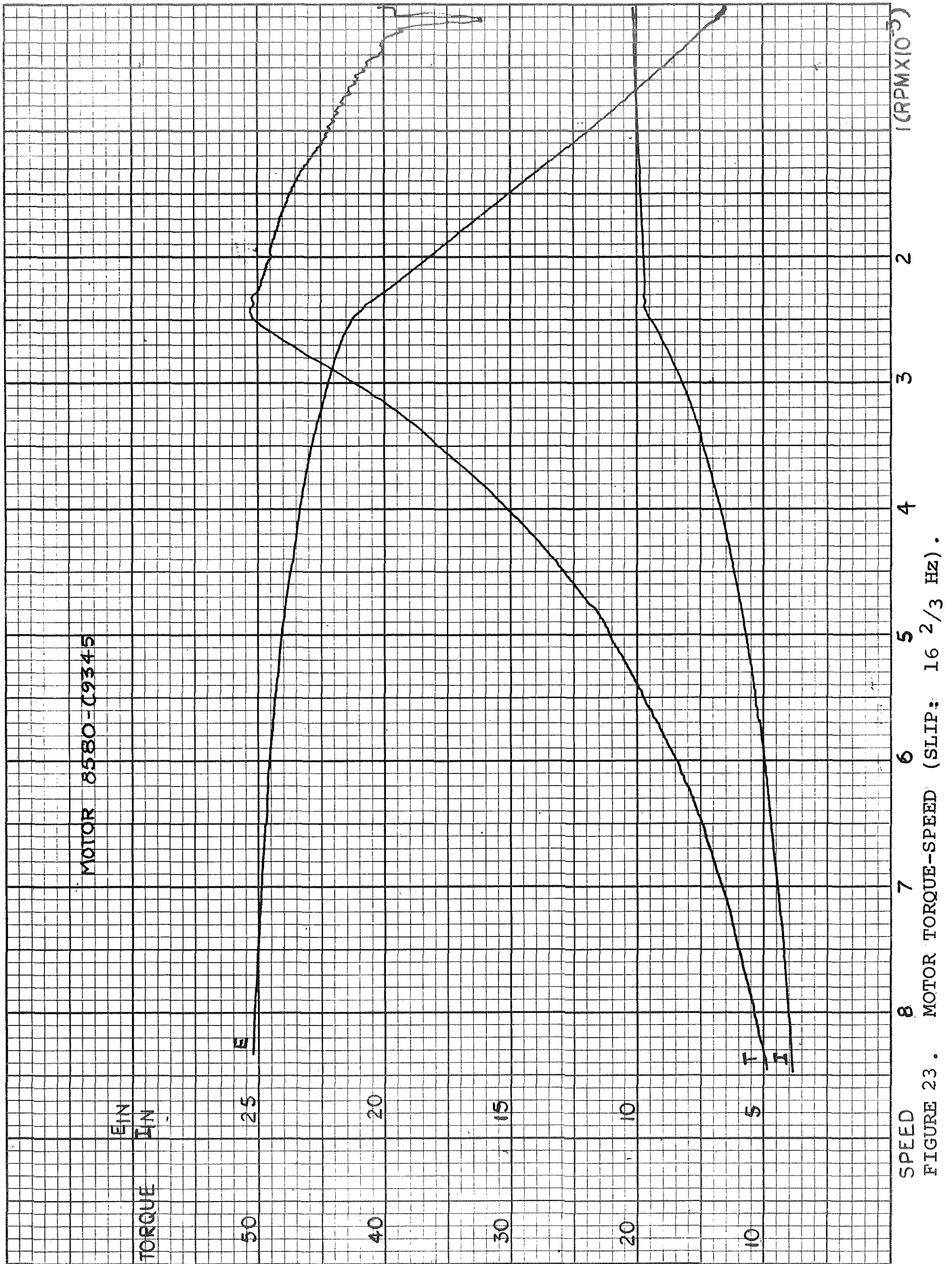
( $V_{in} \approx 25$  VDC)

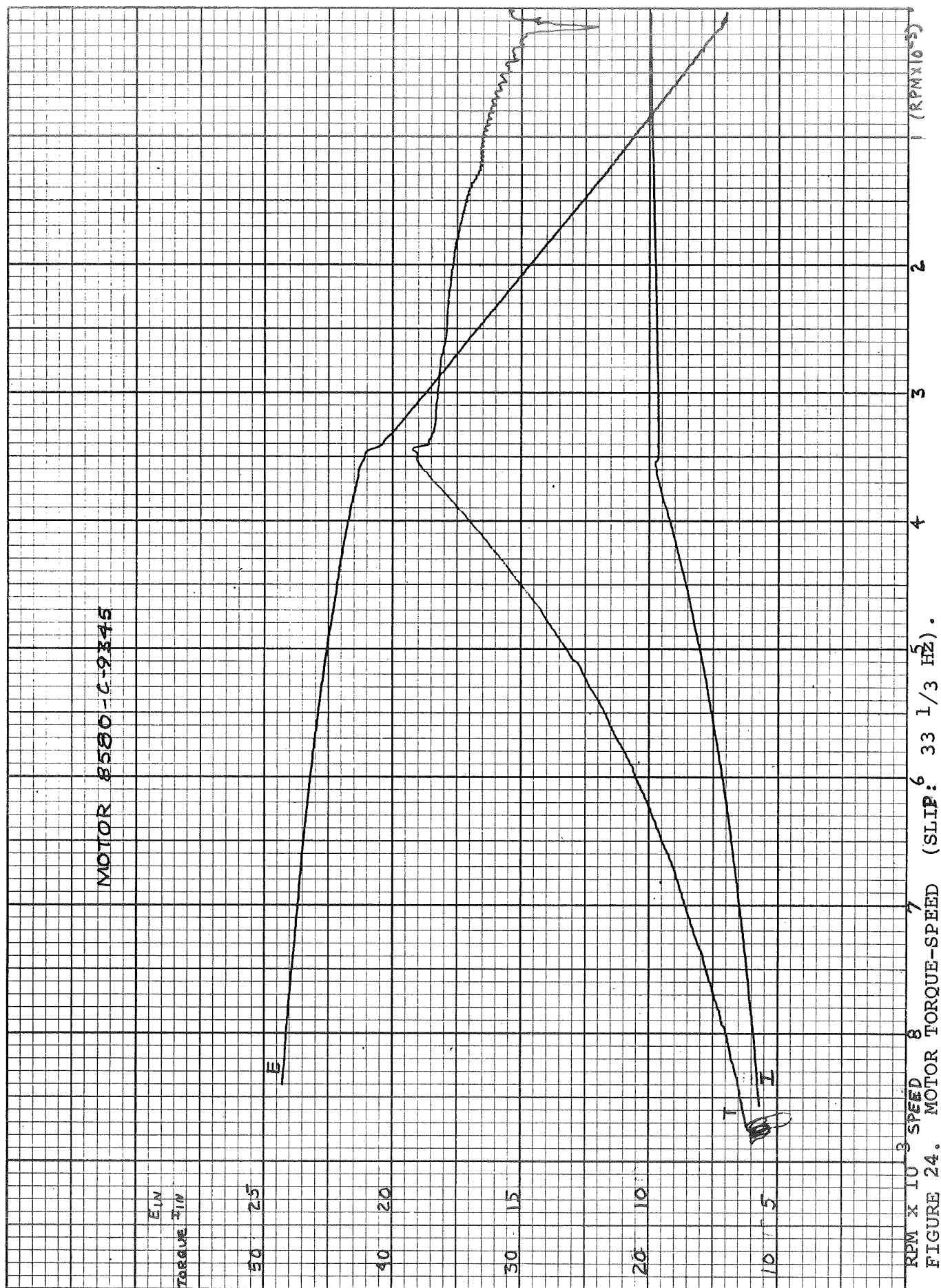
To obtain data with high resolution for the torque-speed tests, the frequency counter was adjusted to present slip indications at 50, 100, and 200 Hz (6 times the actual motor input frequencies). The table above indicates that maximum efficiency during this test occurred at a slip frequency of  $16 \frac{2}{3}$  Hz.

B. Motor Design and Test Results.

A motor consisting of one rotor and two interchangeable field housing assemblies (in effect, two motors), was purchased for this study program. The motor is wound







for three phase, six pole, 400 Hz operation with bifilar windings, and all 12 connecting leads are accessible. One field housing assembly was fabricated with M19 (Silicon Steel) laminations (here-after referred to as Motor No. 1). The alternate field housing assembly was fabricated with Allegheney Ludlum 4750 (Stainless Steel) laminations (here-after referred to as Motor No. 2). Otherwise the two field housing assemblies were identical. Allegheney Ludlum 4750 material was used in an attempt to determine the affect of material in relation to motor efficiency. Test results did not reveal any significant differences of motor efficiency when either material was used.

The winding configuration was designed to permit system testing with either full wave three phase inverter or half wave six phase inverter outputs.

The manufacturers performance data supplied with these motors are presented on Figures 25 and 26.

Inverter-motor system tests included motor operation with a six phase quasi-square wave motor input and six phase square wave motor input (each motor input configuration was applied with and without an interphase transformer) as shown on Figure 27. When input power was applied to the test motor the system increased in speed to a point where the load motor absorbed the power delivered by the test motor. Efficiency was calculated by dividing the load motor shaft output power ( $\text{Watts Power} = 0.00074 \times \text{RPM} \times \text{OZ} - \text{IN TORQUE}$ ) by system input power ( $P = IE$ ). Test measurements obtained at several input power levels are presented on Figure 28. These measurements indicate the following:

1. Maximum efficiency is obtained with a slip of 12 Hz to 20 Hz.
2. Quasi-square wave motor input results in more efficient operation than does a square wave motor input.
3. The interphase transformer improves the efficiency

MOTOR PERFORMANCE CURVES AT 70°F  
 22 VOLTS, 400 HZ, 3 PHASE 6 POLE (M19 SILICON STEEL LAMINATION)

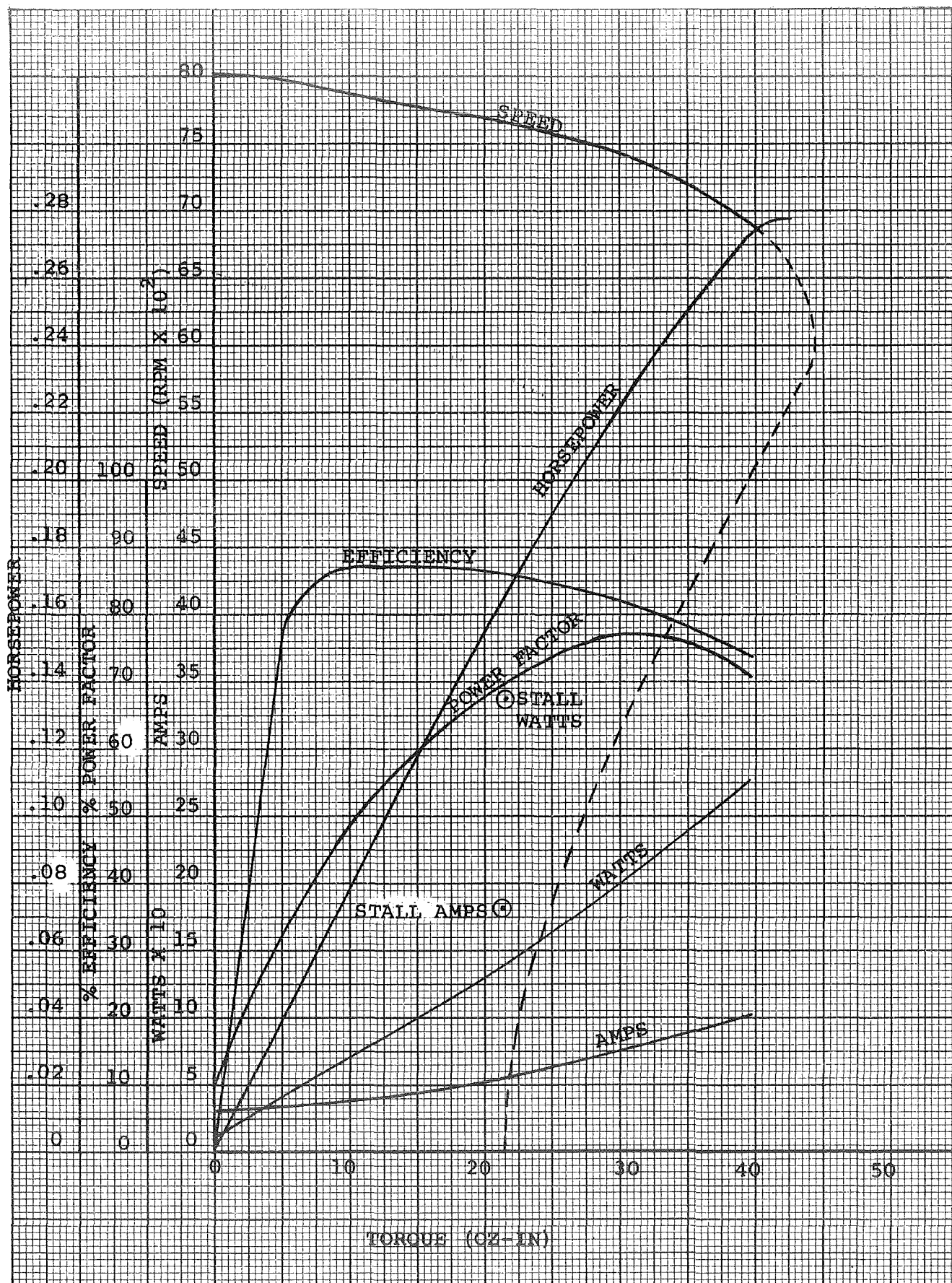


FIGURE 25. MOTOR NO. 1 PERFORMANCE CURVES (MANUFACTURERS DATA) .

MOTOR PERFORMANCE CURVES AT 70°F  
 22 VOLTS, 400 HZ, 3 PHASE 6 POLE (4750 STAINLESS STEEL LAMINATION)

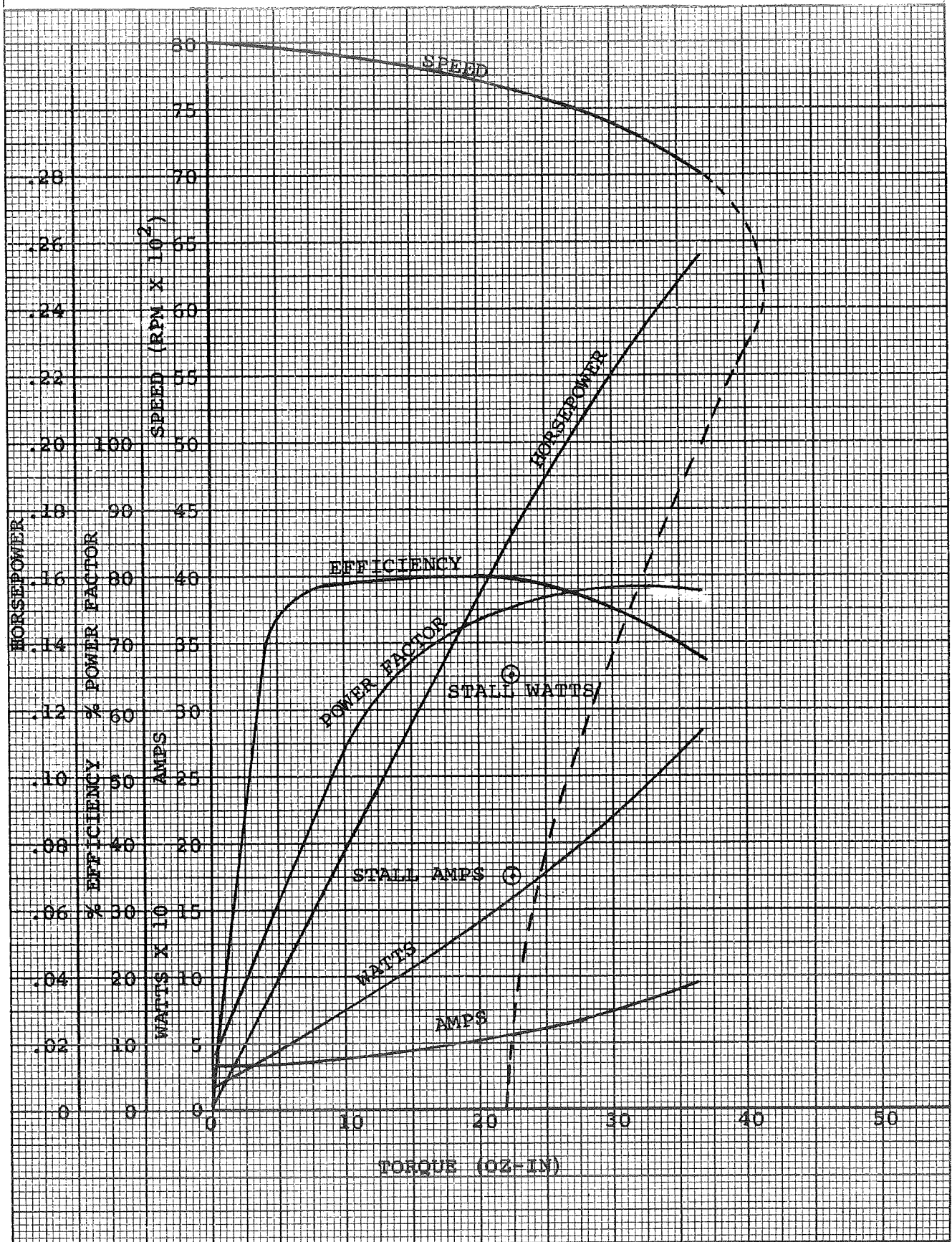


FIGURE 26. MOTOR NO. 2 PERFORMANCE CURVES (MANUFACTURERS DATA).

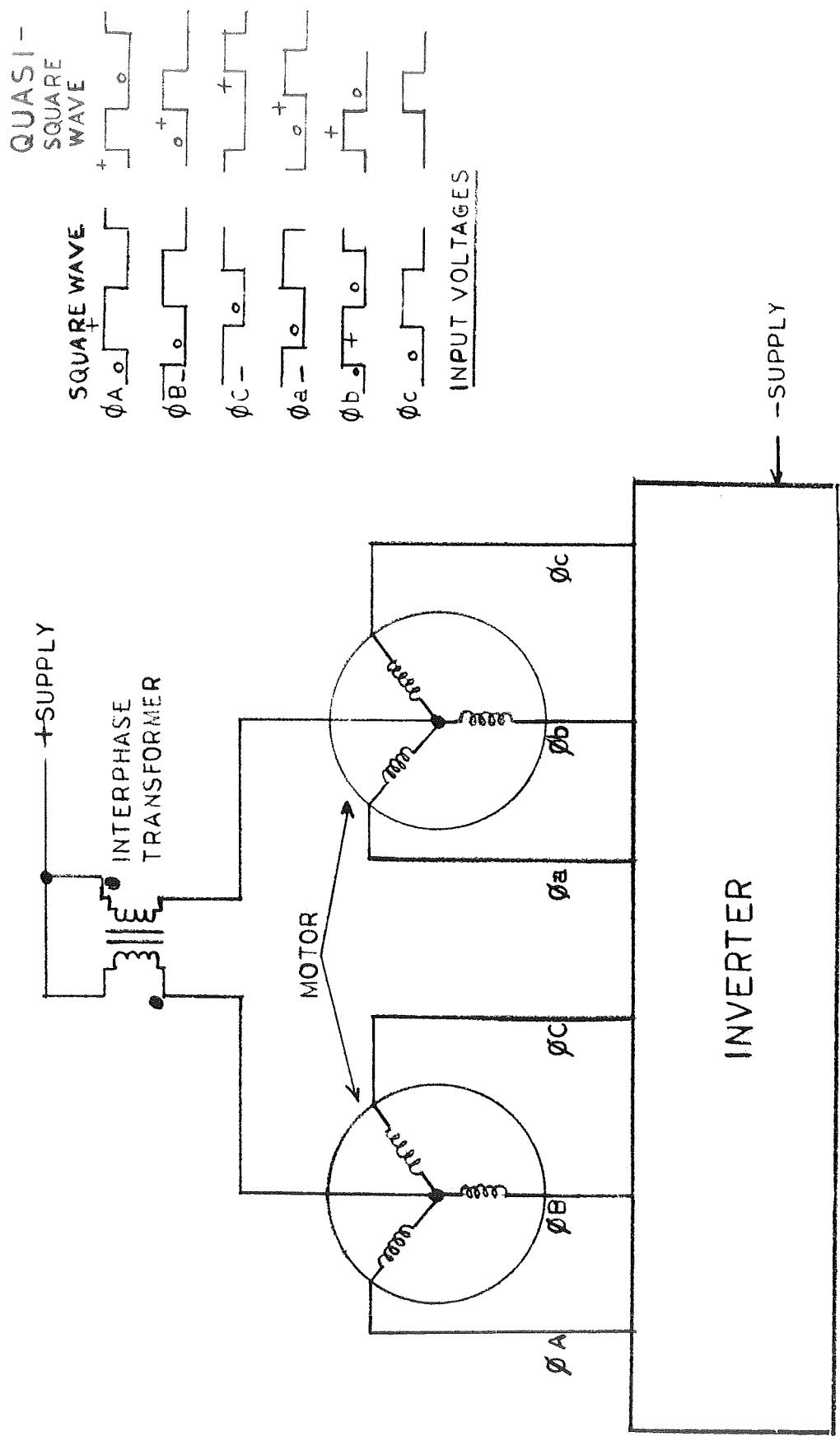


FIGURE 27. SIX PHASE MOTOR INPUT TEST CONNECTIONS.

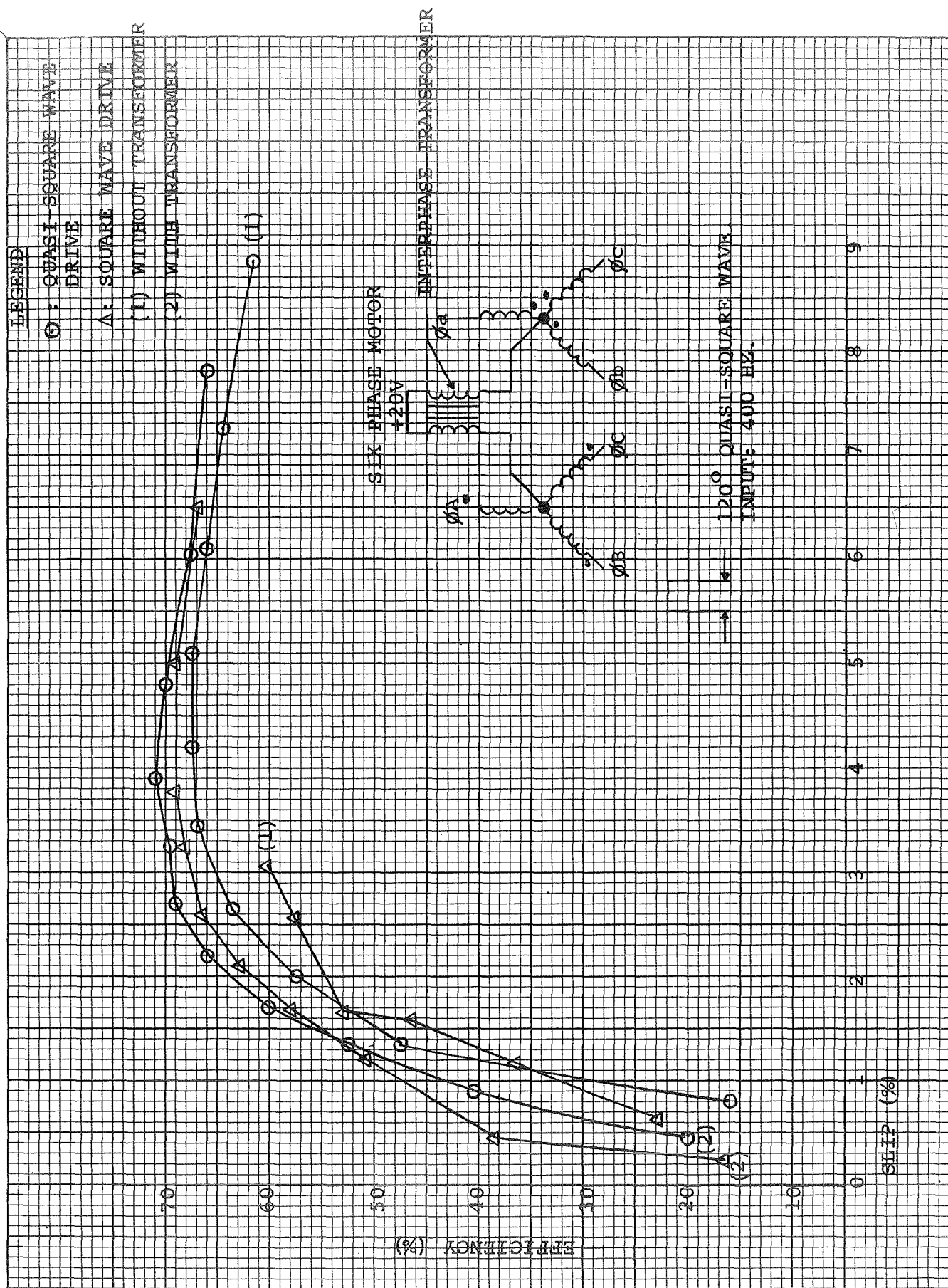


FIGURE 28. EFFICIENCY VS SLIP: 6 $\phi$  SQUARE WAVE AND 6 $\phi$  QUASI-SQUARE WAVE.

of quasi-square wave motor input operation approximately 2%, and improves square wave motor input operation 8 to 10%.

Filtered Output: Three 173 $\mu$  Henry inductors were connected in series with the Inverter output (one inductor to each output lead) to determine the effect of reducing the high frequency current. Two motor (Torque-Speed) operation curves were obtained. One curve was obtained with the inductors connected to the Inverter output. The other curve was obtained with the inductors removed from the Inverter output. The two curves are presented on Figures 29 and 30 respectively. The oscilloscope photographs, Figure 31, are the respective current and voltage waveforms.

The following table compares motor efficiency without filtered Inverter output ( $L=0$ ) vs motor efficiency with filtered Inverter output ( $L=173\mu\text{H}$ ).

MOTOR SPEED (RPM)	EFFICIENCY (%)		EFFICIENCY CHANGE (%) ( $L=173\mu\text{H}$ )
	$L=0$	$L=173\mu\text{H}$	
500	9.8	12.7	+2.9
1000	18.3	23.2	+4.9
2000	32.2	38.2	+6.0
3000	44.3	48.7	+4.4
4000	51.0	54.4	+3.4
5000	60.4	63.8	+3.4
6000	63.2	64.6	+1.4
7000	64.6	62.3	-2.3
8000	65.5	64.0	-1.5
9000	63.7	62.6	-1.1

A major improvement of efficiency was obtained with the added inductors at lower motor speeds. At the higher speeds the added inductance reduces the input current which results in lower efficiency.

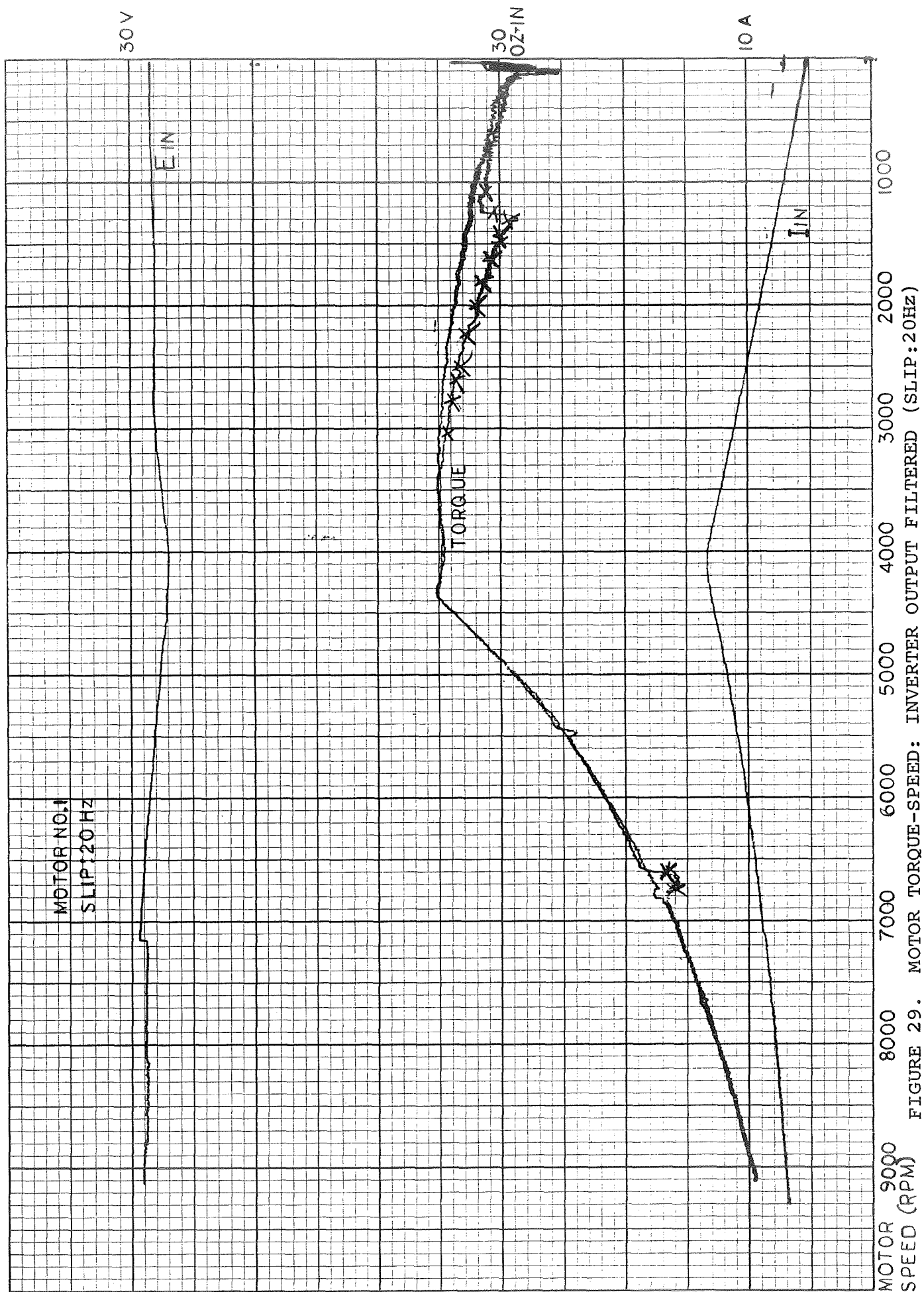
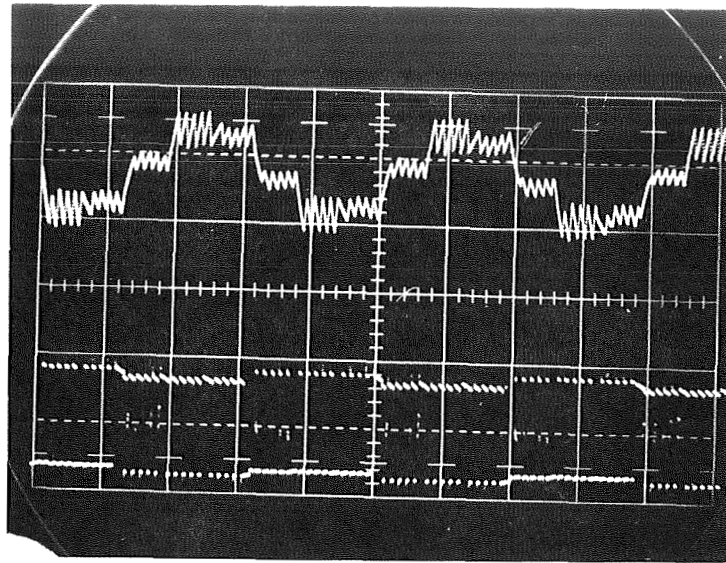


FIGURE 29. MOTOR TORQUE-SPEED: INVERTER OUTPUT FILTERED (SLIP: 20Hz)



FIGURE 30. MOTOR TORQUE-SPEED: INVERTER OUTPUT NOT FILTERED (SLIP: 20Hz)

INVERTER OUTPUT: WITH FILTER

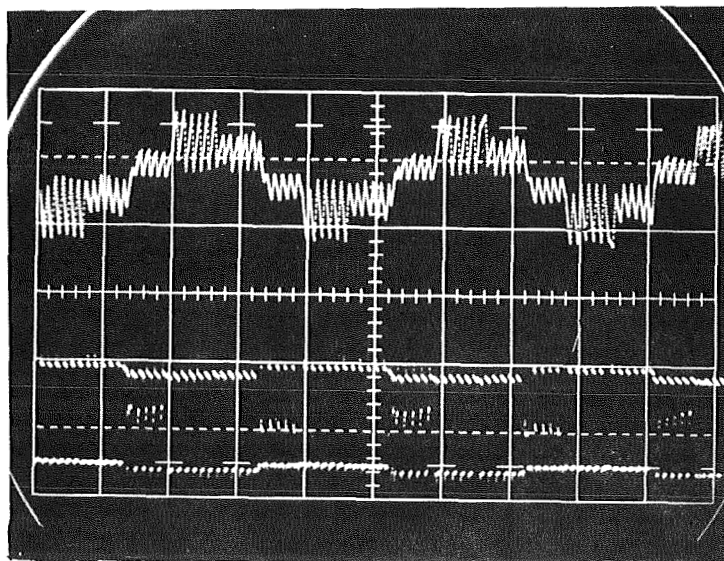


10A/DIV

20V/DIV

200 MS/DIV

INVERTER OUTPUT WITHOUT FILTER



10A/DIV

20V/DIV

200 MS/DIV

FIGURE 31. INVERTER OUTPUT PHOTOGRAPHS

## V. CONCLUSIONS

The information obtained from the Inverter-Motor system tests and from the investigations conducted for this study program is defined in the following paragraphs.

### A. Current Limiting.

To obtain effective variable speed, high efficiency operation of induction type motors, a method of current limiting is required. The system test results show that a current limiting power supply is a sufficient method of current limiting for low power operation (approximately 100 watts), and that pulse width current control methods are more compatible with high power operating requirements (greater than 100 watts). Synchronization of the modulation frequency with the inverter output is not necessary. Other test results obtained during this study program emphasized that most effective motor operation is obtained with the modulation frequency at approximately 24 times the maximum inverter output frequency.

### B. Efficiency.

The pulse width method of current limiting resulted in obtaining an efficiency of 68% with a motor speed of 7000 RPM and a slip of 25Hz. At a motor speed of 4000 RPM and a slip of 25Hz, an efficiency of 56.1% was obtained. The current limiting power supply method of current limiting produced an efficiency of 62% at a motor speed of 6000 RPM and  $16 \frac{2}{3}$  Hz slip, and 57% efficiency at 4000 RPM motor speed with  $16 \frac{2}{3}$  Hz slip.

Greatly increased low speed torque and efficiency is obtained in variable speed operation without an increase in starting current requirements, when constant slip operation is used with variable frequency drive.

### C. Variable Slip.

Variable slip up to the stall torque value is easily implemented into the circuit design, and with minor modifications the slip can be used for braking while maintaining the regenerated braking to a limited value. The use of bifilar wound motors presents definite advantages in respect to the design of inverter output

stages, although more elaborate logic control and more complex motor controls are required for this type of motor.

D. Motor Material.

The use of low-loss material for stator construction does not necessarily result in any measurable advantage over the use of standard stator material.

APPENDIX I

FINAL INVERTER DESIGN  
(THREE PHASE QUASI-SQUARE WAVE OUTPUT)  
AND  
LIST OF MATERIAL





## INVERTER REGULATOR

ELECTRICAL PARTS LIST

MODEL NO. INVERTER-MOTOR

BY D. IRVINE

DATE 4-30-69

PAGE 1 OF 10

QUANTITY	ITEM DESCRIPTION		MANUFACTURER OR MIL. SPEC.	PART NUMBER	ITEM CODE
1	Resistor	2.26K $\Omega$	MEPCO	RN60C2261F	R1
2	"	.5 $\Omega$ $\pm$ 1%	DALE	RS 2B	R2, R3
1	"	7.5 $\Omega$ $\pm$ 1%	DALE	RS-2B	R4
2	"	100 $\Omega$	MEPCO	RN60C1000F	R5, R17
2	"	5110 $\Omega$	MEPCO	RN60C5111F	R6, R22
1	"	30 $\Omega$ $\pm$ 1%	DALE	RS-2B	R7
1	"	180 $\Omega$	MEPCO	RN60C1800F	R8
1	"	.5 $\Omega$ $\pm$ 1%	DALE	RS-2B-4	R9
2	"	2.05K $\Omega$	MEPCO	RN60C2051F	R10, R13
2	"	1K $\Omega$	MEPCO	RN60C1001F	R11, R19
1	"	4.02K $\Omega$	MEPCO	RN60C4021F	R12
1	"	51.1K $\Omega$	MEPCO	RN60C5112F	R14
1	"	.05 $\Omega$ $\pm$ 1%	DALE	RS-2B	R15
1	"	500 $\Omega$	BOURNS	RT12C2L501	R16
1	"	12.1K $\Omega$	MEPCO	RN60C1212F	R18,
2	"	10K $\Omega$	MEPCO	RN60C1002F	R20, R23
1	"	20K $\Omega$ $\pm$ 1%	BOURNS	224L-1-203	R21
1	Capacitor	10K mfd	SAF-T-MIKE	FD5010M	C1
1	"	1800mfd	GULTON	EM75576-16	C2
3	Transistor		RCA	2N3771	Q1, Q2, Q3
1	"		GULTON	EM74709	Q4
2	"		MOTOROLA	2N3801	Q5, Q6
2	"		RAYTHEON	2N2222	Q7, Q9
1	"		GULTON	EM74706	Q8

## INVERTER REGULATOR (cont'd)

ELECTRICAL PARTS LIST

MODEL NO. INVERTER-MOTOR

BY D. Irvine

DATE 4-30-69

PAGE 2 OF 10

QUANTITY	ITEM DESCRIPTION	MANUFACTURER OR MIL. SPEC.	PART NUMBER	ITEM CODE
1	Transistor	GULTON	EM14166-1	Q10
2	Inductor (2 Core)			L1, L2
2	Diode	WESTINGHOUSE	1N3910	CR1, CR2
1	"	GULTON	EM79466	CR3
1	"	TEXAS INSTR.	1N746	CR4
1	"	TRW	PS510	CR5
1	"	GULTON	EM79430	CR6

## SLIP CONTROL

ELECTRICAL PARTS LIST

PAGE 3 OF 10

MODEL NO. INVERTER-MOTOR

BY D. IRVINE

DATE 4-30-69

QUANTITY	ITEM DESCRIPTION	MANUFACTURER OR MIL. SPEC.	PART NUMBER	ITEM CODE
1	Resistor 1.8K $\Omega$	ALLEN BRADLEY	RC05GF182J	R1
2	" 17.8K $\Omega$	MEPCO	RN55C1782F	R2, R3
11	" 10.5K $\Omega$	CORNING	RN55C1052F	R4, R7, R9, R12, R13, R14, R19 R20, R21, R23, R28
1	" 1.1K ohms	CORNING	RN55C1101F	R5
1	" 1K $\Omega$	CORNING	RN55C1000F	R6
2	" 1K $\Omega$ Linear Potentiometer	SPECTROL	Model 510	R8, R25
1	" 4.02K $\Omega$	CORNING	RN55C4021F	R10
2	" 1.96K $\Omega$	CORNING	RN55C1961F	R11, R18
2	" 4.87K $\Omega$	CORNING	RN55C4871F	R15; 26
3	" 1.5K $\Omega$	ALLEN BRADLEY	RC05GF152J	R16, R29, R16A
1	" 4.02K	CORNING	RN55C4021F	R17
1	" 110K $\Omega$	CORNING	RN55C1103F	R22
2	" 169 $\Omega$	CORNING	RN55C1690F	R24, R27
1	" 51.1 $\Omega$	CORNING	RN55C51R1F	R30
2	" 4.7K $\Omega$	ALLEN BRADLEY	RC05GF472J	R31, R32
3	" 10K $\Omega$	ALLEN BRADLEY	RC05GF103J	R33, R34, R38
2	" 33K $\Omega$	ALLEN BRADLEY	RC05GF333J	R35, R37
1	" 100 $\Omega$	ALLEN BRADLEY	RC05GF101J	R36
1	" 2.2K $\Omega$	ALLEN BRADLEY	RC05GF222J	R39
1	" 10K $\Omega$	BOURNS	RT12C22103	R40
1	" 1.2K $\Omega$	ALLEN BRADLEY	RC05GF122J	R41

## SLIP CONTROL (Cont'd)

ELECTRICAL PARTS LIST

PAGE 4 OF 10

MODEL NO. INVERTER-MOTOR

BY D. IRVINE

DATE 4-30-69

QUANTITY	ITEM DESCRIPTION		MANUFACTURER OR MIL. SPEC.	PART NUMBER	ITEM CODE
1	Resistor	250K $\Omega$ Linear Potentiometer	CTS	PO11-130	R42
1	"	5.7K $\Omega$	ALLEN BRADLEY	RC05GF572J	R43
1	"	226 $\Omega$	CORNING	RN55C2260F	R44
1	"	154 $\Omega$	CORNING	RN55C1540F	R45
2	Capacitor	.033mfd	ELECTROCUBE	EC1625B	C1,C5
2	"	2.2mfd	KEMET	CS12BE225M	C2,C6
3	"	.0047mfd	ELECTROCUBE	EC1625B472J	C3,C8, C3A
2	"	221pfd	KEMET	CX12AX221M	C4,C9
1	"	1mfd	ELECTROCUBE	EC1625B1B105J	C7
1	"	.01mfd	ELECTROCUBE	EC1625B103J	C10
1	Transistor		FAIRCHILD	2N2452	Q1
2	"		MOTOROLA	2N2923	Q2,Q3
2	"		RAYTHEON	2N2222	Q4,Q5
2	"		MOTOROLA	2N4401	Q6,Q7
1	"		MOTOROLA	2N4403	Q8
1	"		MOTOROLA	2N4852	Q9
2	"		FAIRCHILD	9601	Z1,Z3
2	"		FAIRCHILD	709	Z2,Z4
1	"		FAIRCHILD	946	Z5
2	"		FAIRCHILD	945	Z6,Z7
2	Diode		TEXAS INSTR	1N745A	CR1,CR2
2	DIODE		TEXAS INSTR	1N645	CR3,CR4
1	Switch		ALCO	MST105D	S1
1	Switch		ALCO	MST205N	S2

DC TO DC CONVERTER  
ELECTRICAL PARTS LIST



MODEL NO. INVERTER-MOTOR

BY D. IRVINE

DATE 4-30-69

PAGE 5 OF 10

QUANTITY	ITEM DESCRIPTION	MANUFACTURER OR MIL. SPEC.	PART NUMBER	ITEM CODE
1	Transformer	---	---	T1
1	Resistor 15Ω ±1%	DALE	RS-2B	R1
1	Resistor 1KΩ	MEPCO	RN60C1003F	R2
2	Transistor	RCA	2N3585	Q1, Q2
3	Diode	TEXAS INSTR	1N645	CR1, CR2, CR4
1	"	MOTOROLA	M4L3054	CR3
2	"	WESTINGHOUSE	1N1202A	CR5, CR6
6	"	WESTINGHOUSE	1N4818	CR7, CR8, CR9 CR10, CR11, CR12
2	"	TEXAS INSTR	1N4002	CR13, CR14
1	Capacitor 1mfd	GULTON	EM77308-3	C1
5	Capacitor 47mfd	KEMET	CS12BF476	C2, C3, C5, C6, C7
1	Capacitor 1mfd	KEMET	CS12BF105M	C4

# CONVERTER REGULATOR

## ELECTRICAL PARTS LIST



MODEL NO. INVERTER-MOTOR

BY D. IRVINE

DATE 4-30-69

PAGE 6 OF 10

QUANTITY	ITEM DESCRIPTION	MANUFACTURER OR MIL. SPEC.	PART NUMBER	ITEM CODE
1	Resistor 5.11KΩ	CORNING	RN55C5111F	R1
1	" 1.05KΩ	CORNING	RN55C1051F	R2
1	" 6.19KΩ	CORNING	RN55C6191F	R3
1	" S-1-T	CORNING	RN55C(S-1-T)	R4
1	" 1.54KΩ	MEPCO	RN55C1541	R5
1	Transistor	RCA	2N3772	Q1
2	Transistor	GULTON	EM74706	Q2, Q4
1	Transistor	GULTON	EM74709	Q3
1	Diode	TEXAS INSTR	1N746A	CR1
1	Diode	TEXAS INSTR	1N753A	CR2
1	Capacitor 47mfd	KEMET	JAN M390031 01-2072	C1
1	Capacitor .01mfd	ELECTRO-CUBE	EC1-210C	C2

OUTPUT SECTION  
ELECTRICAL PARTS LIST



MODEL NO. INVERTER-MOTOR

BY D. IRVINE

DATE 4-30-69

PAGE 7 OF 10

QUANTITY	ITEM DESCRIPTION		MANUFACTURER OR MIL. SPEC.	PART NUMBER	ITEM CODE
6	Resistor	1K $\Omega$ $\pm$ 1%	ALLEN BRADLEY	RC05	R101,R103,R105 R110,R113,R116
6	"	470 $\Omega$ $\pm$ 1%	ALLEN BRADLEY	RC05	R102,R104,R106 R111,R114,R117
6	"	330 $\Omega$ $\pm$ 1%	ALLEN BRADLEY	RC05	R107,R108,R109 R112,R115,R118
6	Resistor	1.2K $\Omega$ $\pm$ 1%	ALLEN BRADLEY	RC05	R119,R120,R121 R122,R123,R124
12	Transistor		GULTON	EM73531	Q101,Q104,Q107 Q110,Q113,Q116, Q119,Q120,Q121 Q122,Q123,Q124
6	"		MOTOROLA	2N4233	Q102,Q105,Q108 Q111,Q114,Q117
6	"		RCA	37984	Q103,Q106,Q109 Q112,Q115,Q118
6	Diode		GULTON	EM748081	CR101,CR102 CR103,CR104 CR105,CR106
	"				

## PULSE WIDTH CURRENT CONTROL

ELECTRICAL PARTS LIST

PAGE 8 OF 10

MODEL NO. INVERTER-MOTOR

BY D. IRVINE

DATE 4-30-69

QUANTITY	ITEM DESCRIPTION		MANUFACTURER OR MIL. SPEC.	PART NUMBER	ITEM CODE
1	Resistor	.02Ω±1%	DALE	RS2B	R125
1	"	20Ω±1%	DALE	RS2B	R126
2	"	1KΩ	CORNING	RN55C1001F	R127 R128
1	"	9.53KΩ	CORNING	RN55C9531F	R129
1	"	20KΩ	CORNING	RN55C2002F	R130
1	"	1.5KΩ ±1%	ALLEN BRADLEY	RC05	R131
1	"	25KΩ Linear Potentiometer	ALLEN BRADLEY	CU2531	R132
3	"	10KΩ	CORNING	RN55C1002F	R133, R134, R135
2	"	6.19KΩ	CORNING	RN55C6191F	R136, R143
1	"	4.64KΩ	CORNING	RN55C4641F	R137
1	"	5.11KΩ	CORNING	RN55C5111F	R138
1	"	215Ω	MEPCO	RN60C2150F	R139
2	"	27KΩ ±1%	ALLEN BRADLEY	RC05	R140, R142
1	"	154Ω	CORNING	RN55C1540F	R144
1	"	250K linear Potentiometer	CTS	P011-130	R145
1	"	4.02KΩ	MEPCO	RN60C4021F	R146
1	"	220Ω ±1%	ALLEN BRADLEY	RC05	R147
1	"	150Ω ±1%	ALLEN BRADLEY	RC05	R148
1	"	22.6KΩ	ALLEN BRADLEY	RC052262F	R149
1	"	205Ω	CORNING	RN55C2050F	R150
1	Capacitor	22pfd	GULTON	78354-220MH	C101
1	"	471pfd	KEMET	CK12AX471M	C102

I-10

## PULSE WIDTH CURRENT CONTROL (cont'd)

ELECTRICAL PARTS LIST

PAGE 90F10

MODEL NO. INVERTER-MOTOR

BY D. IRVINE

DATE 4-30-69

QUANTITY	ITEM DESCRIPTION	MANUFACTURER OR MIL. SPEC.	PART NUMBER	ITEM CODE
1	Capacitor 47mfd	KEMET	CS12BF476	C103
1	" 1000pfd±1%	AEROVOX	MC70	C104
1	" .01mfd	ELECTROCUBE	EC1-210C	C105
1	" 5mfd	ELECTROCUBE	210C1B505M	C106
2	" .1mfd ±1%	MARSHALL	M2-19	C107, C108
1	Switch	ALCO	MST205N	S102
3	Transistor	MOTOROLA	2N4401	Q125, Q126, Q130
1	"	MOTOROLA	2N4403	Q127
1	"	MOTOROLA	2N4852	Q128
1	"	GULTON	EM79458	Q129
1	Integrated Circuit	FAIRCHILD	709	Z101
1	"	FAIRCHILD	945	Z102
1	"	FAIRCHILD	946	Z110

RING COUNTER CIRCUIT  
 ROTATION AND CURRENT  
 MODULATION GATES  
ELECTRICAL PARTS LIST



MODEL NO. INVERTER-MOTOR

BY D. IRVINE

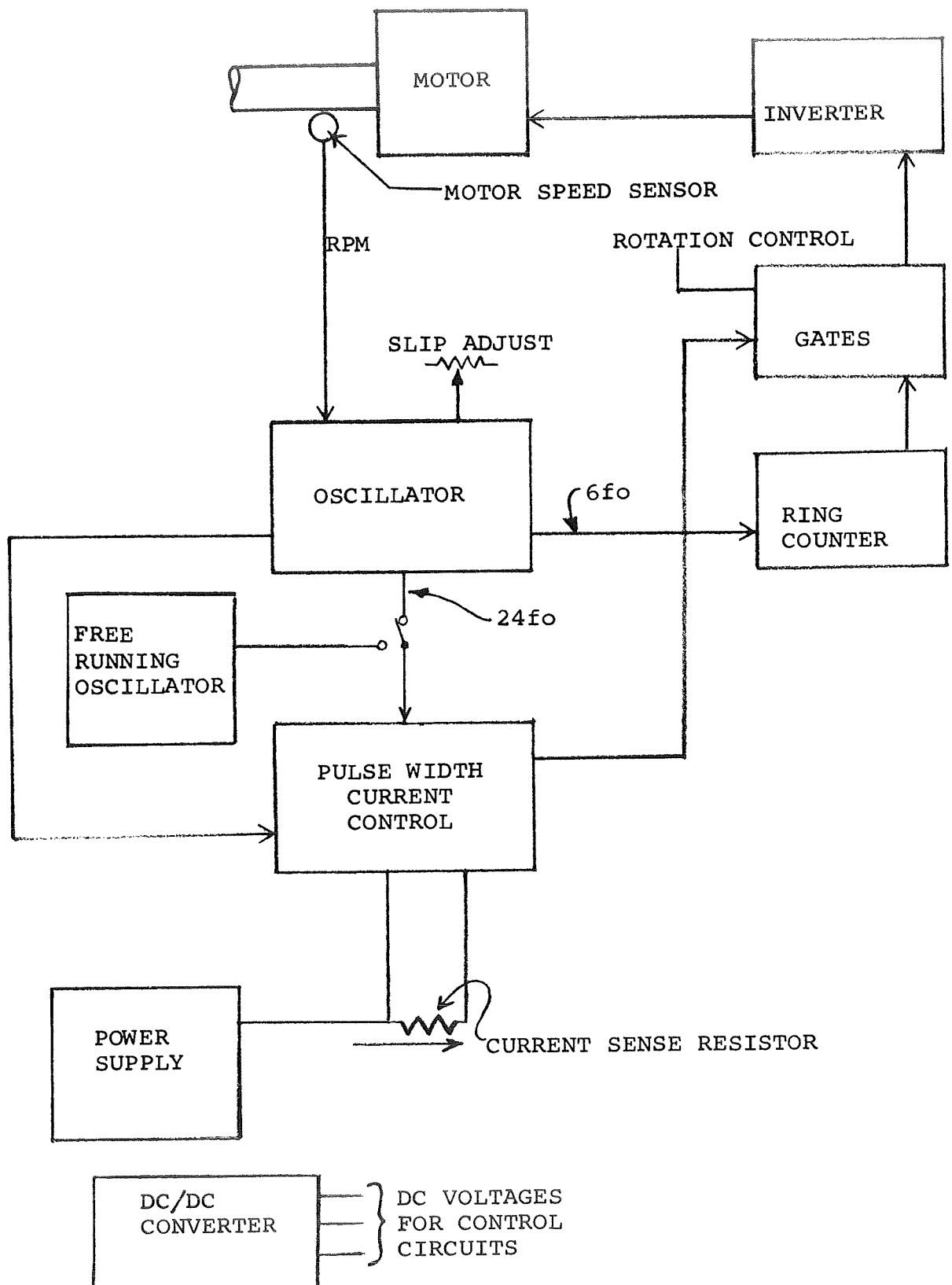
DATE 4-30-69

PAGE 1 OF 10

QUANTITY	ITEM DESCRIPTION	MANUFACTURER OR MIL. SPEC.	PART NUMBER	ITEM CODE
	<u>RING COUNTER</u>			
3	Integrated Circuit Flip Flop	FAIRCHILD	945	Z107,108,109
	<u>ROTATION AND CURRENT MODULATION GATES</u>			
1	Integrated Circuit	FAIRCHILD	946	Z103
3	"	FAIRCHILD	962	Z104,Z105,Z106
1	Switch	ALCO	MST105D	S1

APPENDIX II

BLOCK DIAGRAM OF INVERTER BREADBOARD



BLOCK DIAGRAM OF INVERTER BREADBOARD.